Exploration of shallow sandy ridge systems for aquifer storage and recovery solutions in the Vietnamese Mekong Delta

Utrecht University MSc. Thesis

Josh Shankel

A field study in the Tra Vinh and Ben Tre provinces, Mekong Delta, Vietnam

By

Josh Shankel

in partial fulfilment of Master of Earth Sciences degree in Earth Surface & Water from Utrecht University

Supervisors: Dr. Philip Minderhoud & Dr. Gualbert Oude Essink

Name: Josh Shankel
Student ID: 6385109
Email: j.p.shankel@students.uu.nl
Faculty of Geoscience, Utrecht University

Abstract

Especially in recent years, the Vietnamese Mekong delta has experienced extreme saltwater intrusion, affecting surface waters further inland than ever before, causing hundreds of millions of dollars in damage. Due to the desired economic growth of the Vietnamese Mekong Delta, fresh groundwater resources are intensively exploited to meet up water demand needed for food, domestic use and industrial activities. The food productivity of the Mekong Delta responsible for 50% of the food supply of Vietnam. The over exploitation of the water resources causes freshwater scarcity which leads to land subsidence and saltwater intrusion of both groundwater and surface water. In this study, a solution to shallow ground water scarcity is investigated. Here, the feasibility of an aquifer storage and recovery (ASR) solution is evaluated. focussing on shallow phreatic sandy ridge aquifers in the provinces of Tra Vinh and Ben Tre in the Mekong Delta in Vietnam. These solutions have been successful in the Netherlands on similar geomorphological features, and thus, it is investigated if the implementation of these systems could also be a promising way to provide freshwater security in the Mekong Delta, Vietnam. An analysis of the geological architecture of the sandy ridge structures was explored during a three-month field campaign at three potential sites. Using shallow suction coring, deep coring and cross section analysis, the sandy ridges were evaluated in terms of lithology, storage capacity, and ultimately, feasibility for an ASR solution. At least one such site in the province of Ben Tre shows future potential of an ASR pilot. A suitability map was developed to upscale the potential of additional sites in the two investigated provinces that could benefit the most from an ASR system. Zones with sandy ridge structures, that irrigate during the dry season and experience saltwater intrusion into the surface water systems stand to be the areas that can benefit the most from an ASR system. With increasing water demand, expanding innovative water management techniques is an important component moving towards a more sustainable future of the supply of freshwater and food in the Vietnamese Mekong Delta.

Acknowledgements

This thesis provided me the opportunity to learn how to conduct my own research in hands on environment. The field work in Vietnam was an incredible experience and I have many collogues and friends to thank for their help and collaboration, in making this study an invaluable learning opportunity. Through this research I have gained valuable insight into applied research, new concepts in the field of geoscience and hydrogeology, and a fascinating new country and culture.

I would like to thank Deltares for supporting this project and my field work. I would like to thank my supervisors Philip Minderhoud and Gualbert Oude Essink for guiding our field team as we completed our work in Vietnam, and for their patience and support throughout completion of my thesis. Sep Bregman and Anne Kruijt were invaluable partners and friends and this project would not have been possible without their collaboration and camaraderie. A special thanks to Geoff Zimmel for preparing us for our campaign and supporting our efforts from afar, and to Dr. Nguyen Hong Quan for aiding us during the exploration of our field sites and connecting us with his network of collaborators and interpreters.

The completion of this thesis was greatly aided by the efforts of; Stan Schouten for his MATLAB expertise, Guillermo Molina for his help with map processing, Tim Winkels and Pieter Pauw forteaching us proper field techniques, and Sepehr Eslami for sharing data from his surface water models.

With this MSc thesis I hope I can provide some insight into some of the water security issues facing many of the people in the Vietnamese Mekong Delta, and work towards some potential solutions. I had the unique pleasure of being able to meet so many interesting and friendly during my time there in the Mekong Delta. Thank you for your hospitality.

Table of Contents

1 Introduction

In the 4th Intergovernmental Panel on Climate Change (IPCC) report of 2007, mega deltas were identified as one of the most vulnerable environments endangered by human activity and climate change (Foufoula-Georgiou, 2013). Deltas are characterized as low ling coastal land forms sculpted by the interplay of rivers, tidal and wave processes (Wong et al. 2014). Deltas are highly sensitive to changes from the upstream fresh water inputs and downstream oceanic changes in tide, waves, and sea level. They are also highly impacted by human activities such as; urbanization, land use change, subsurface resource extraction, upstream dam construction, and irrigation (Nicholls et al., 2007). The IPCC report of 2014 places a very high confidence on the widespread degradation of deltas world-wide (Wong et al. 2014). This is very concerning considering deltas are home to many major cities and valuable expanding economies. Deltas are also very valuable productive areas globally, supporting much of the world's agriculture, fisheries, and forestry products (Foufoula-Georgiou, 2013). The value of deltas globally expands far beyond their borders. A shift towards sustainability cannot be understated as deltas face continued threats from relative sea level rise, cyclones, river flooding, storm surges, urban expansion, pollution, reduced sediment input, land subsidence, agricultural exploitation, and salinization of fresh waters (Foufoula-Georgiou, 2013).

In the agricultural areas of densely populated deltas, the salinization of fresh water resources has major consequences on food security, livelihoods and health of inhabitants (Rahman et al., 2019). Salt contamination of freshwater sources can cause reduced agricultural productivity, crop losses, ecological damage, and loss of safe drinking water. Salt water intrusions are exacerbated in deltas by human included land subsidence, relative sea level rise, and groundwater abstraction (Rahman et al., 2019). Climate change induced sea level rise often works in tandem with groundwater pumping rates, affecting the fresh and saline groundwater distribution. In low lying coastal zones and deltaic areas, the volume of fresh groundwater storage is under stress, caused by saltwater intrusion. According to the IPCC report of 2014, even smaller extraction rates from coastal aquifers are expected to cause stronger salinization to coastal aquifers than sea level rise (Jiménez Cisneros et al., 2014).

1.1 Study Area: The Vietnamese Mekong Delta

Recent economic growth, population expansion, increased agriculture, salinization and erosion have exposed water supply vulnerabilities in the Vietnamese Mekong Delta (VMD). The VMD is a critical component of the Vietnam's economy and food security as it is responsible for 50% of the country's food production and grows 90% of the rice in Vietnam (GSO, 2016). The Mekong Delta is also the home to 21 million people, and is the most productive agricultural and fishery region in Vietnam, with 65% of the Mekong Delta being used for agriculture (Boretti, 2020). The delta has seen an upward trend in exploitation of groundwater resources for domestic, industrial and agricultural use, leading to declining hydraulic head in the aquifers (Minderhoud et al, 2017). This freshwater demand is only expected to increase. The agricultural demand for 2100 is expected to be three times as high as it was in the year 2000 (Hamer et al., 2020). With overexploitation of the fresh groundwater resources, the delta also faces accompanying pressures that negatively affect water security.

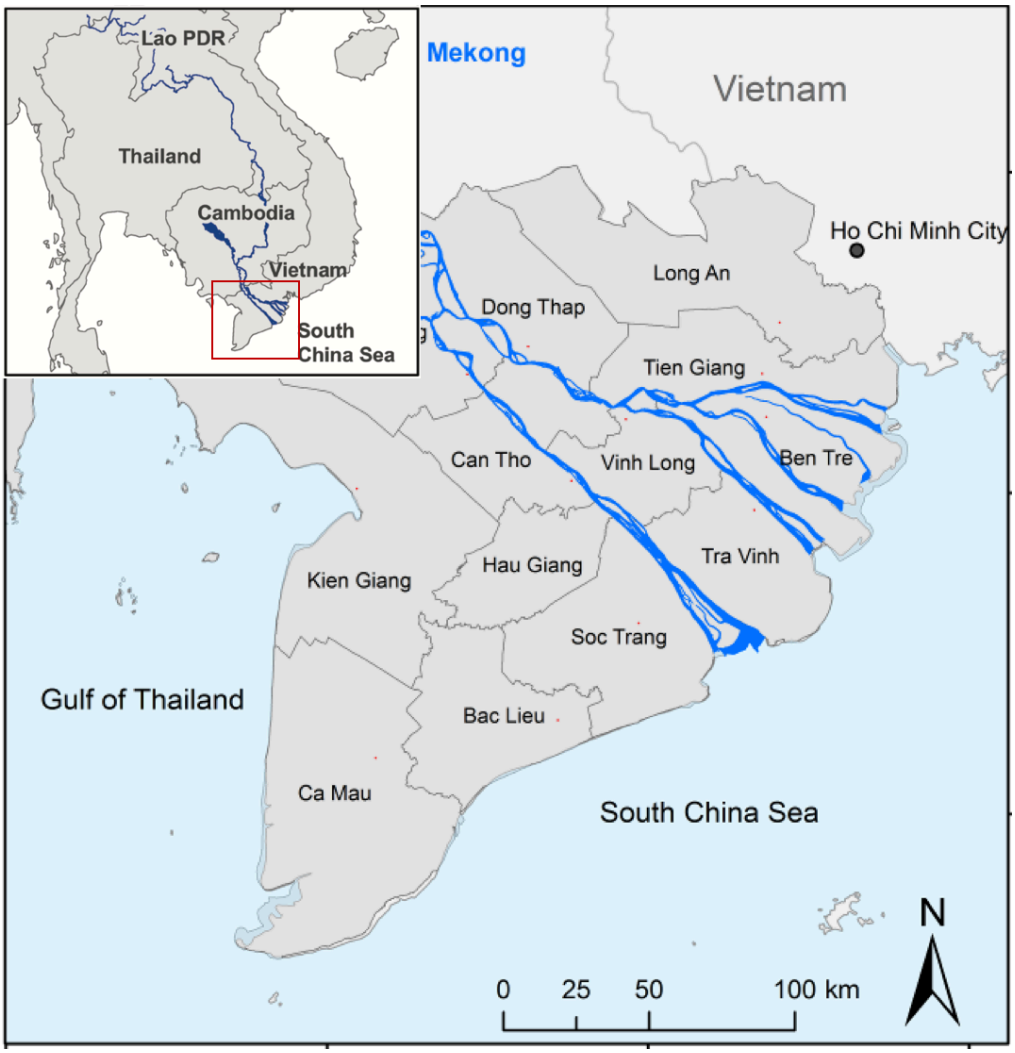

Figure 1 Map showing the Vietnamese Mekong River branches and the extent of the Delta and its provinces (Kuenzer et al., 2013)(Käkönen, 2008).

In the VMD, climate change only serves to exacerbate anthropogenic induced pressures. In the 2015-2016 dry season, the delta suffered an extreme drought and accompanying salt water intrusion. Many canals and dykes were built in the MKD to provide fresh water for irrigation to farmers, but this network has also enabled a pathway for more salt water to come inland during intense intrusive events like storm surges (Rahman et al., 2019). 2016 was the first time the salt water intruded beyond the dykes (CGIAR, 2016). This event was caused by low discharge from the Mekong river and below average precipitation (Sebastian et al., 2016). There were heavy crop losses, and total damages of agriculture and aquaculture were estimated to be 300 million USD (Nguyen, 2017). Events like this have a severe socioeconomic impact on the whole of the Mekong Delta, and put the livelihood of its residence at risk (Nguyen, 2017).

A much more pressing issue than climate change for the delta is human induced subsidence, caused by over exploitation of the groundwater resources. In the Mekong Delta, rates of land subsidence exceed the rate of global sea level rise by an order of magnitude. The global sea level is rising at ~3 mm per year, while the Mekong Delta is currently sinking at an average rate of 11

mm per year, with rates much higher in specific regions (Minderhoud et al., 2017). The scope of this sinking over the past 25 years, is depicted in Figure 2. Declines in hydraulic head from groundwater extraction cause compaction within the aquifers. Every day over 2 million m^3 is pumped from the first 500m of the subsurface (Minderhoud et al., 2015). This is alarming considering that the mean elevation of the Mekong Delta is approximately 0.8 meters above mean sea level (Minderhoud et al., 2019).

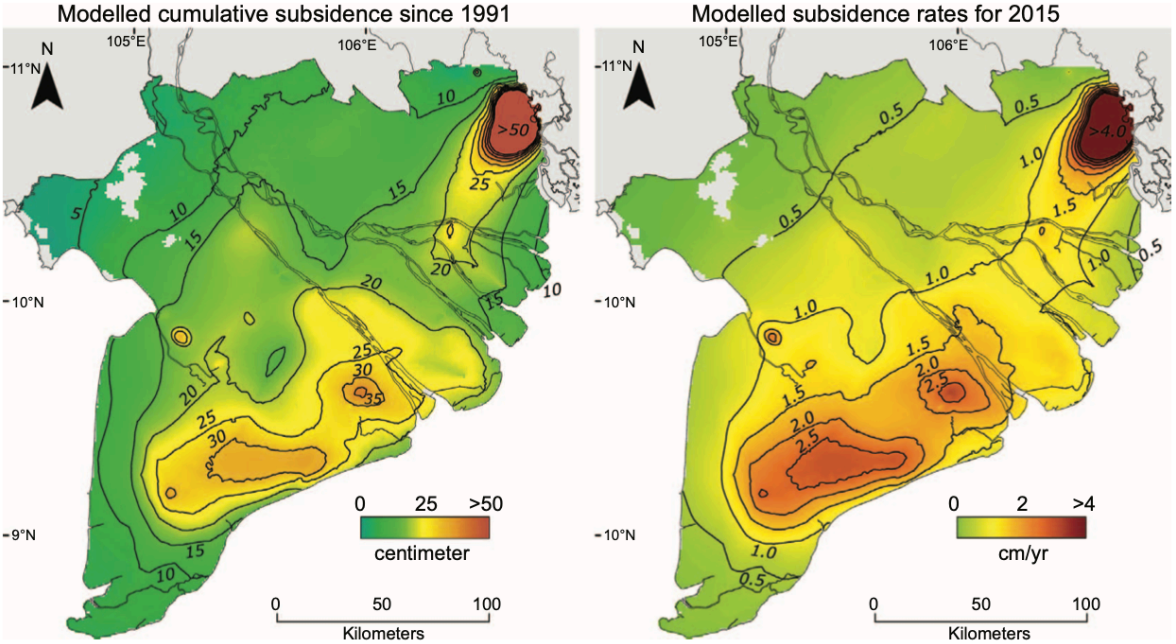

Figure 2 Model outputs of the Mekong Delta showing 25 years of extraction induced subsidence (left), and extraction induced rates of subsidence for 2015 (Minderhoud et al., 2017).

The lowering of the land makes the MKD even more vulnerable to floods, storm surges and saltwater intrusion. This is concerning because, the rural areas of the Mekong Delta, which house Vietnams agricultural production, are being increasingly converted into more groundwater intensive irrigation practices (Minderhoud et al., 2017).

Saltwater intrusions occur not only on the coasts, but also flow upstream through channels reaching further inland (Eslami et al., 2019). During the wet season (July – October) the salt water intrusions are limited, reaching only a few kilometers inland, but in the dry season (December – May) the salt waters can intrude tens of km reaching 1.3 million hectares (Eslami et al., 2019). Salinity problems in the groundwater system are expected to increase with increased groundwater extraction, sea level rise, river discharge changes due to climate change and upstream damming projects (Renaud et al., 2015). In terms of salt water intrusions, the climate change induced sea level rise is surpassed by the deepening of the channels by human activity. The sediment supply upstream is reduced by damming and it is reduced downstream by sand mining, leading to lower bed levels in the channels (Eslami et al., 2019). The construction of dykes and sluice gates has allowed for increased protection from salinity and an increase in water availability for rice crops. This is also creates a problem, as these systems accumulate pollution when the gates close (Renaud et al., 2015). The gates are closed in response to saltwater intrusion of the surface water system. When saltwater intrusions occur more frequently, the surface waters become more unavailable / unusable. With the surface water becoming more

degraded, groundwater extraction is the primary alternative to meet water needs for irrigation (Wagner et al., 2012).

I like ASR on top of the things mentioned above as it uses the subsurface, it uses the abundant surplus during the wet season. This is the winning narrative of ASR you need to mention in the ABSTRACT too. I believe there is no solution that fits all, and they need every possibility to release the system.

1.2 Aquifer Storage and Recovery

This thesis aims to contribute to adaptations that will help conserve freshwater in the MKD. One such way groundwater can be conserved and push back against saltwater intrusion is through aquifer storage and recovery systems (ASR). The function of aquifer storage and recovery systems is to infiltrate freshwater into an aquifer in times of water surplus for storage. The water can then be recovered during times of high demand (Zuurbier et al., 2015). These systems can reduce water supply shortages during periods of very high demand, like droughts. ASR acts as an alternative to the construction of surface water storage projects. As the reservoir is already in the subsurface, the set-up is cost effective, only requires a small amount of land surface, and reduces evaporation loss, compared to an above ground reservoir. ASR systems can also help improve water quality and prevent salt groundwater from intruding into the groundwater system (Rambags et al., 2013).

The shallow sandy ridges in the MKD are the target unconfined aquifers of this study. These sandy ridges are geomorphologically similar to sandy creek ridges in The Netherlands, which have been utilized in the past as ASR sites (Figure 3). The creek ridges are sandy geomorphological features that are elevated up to 2m above the average surrounding ground surface (Pauw et al., 2015). During creek ridge infiltration, water is injected into the aquifer during the wet season, utilizing the excess precipitation with a dedicated infiltration system and a nearby surface water channel. This grows the freshwater lens and increases the water storage volume which can be extracted for irrigation when it is most needed. (Delsman et al., 2015;Oude Essink et al.,2014, 2018).

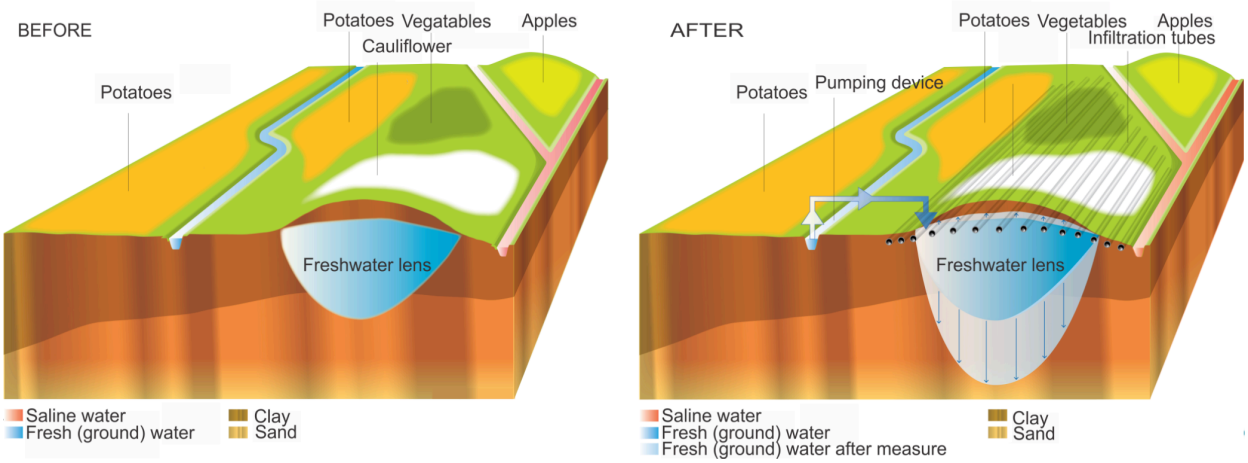

Figure 3 Extension of a freshwater lens using creek ridge infiltration to increase freshwater storage .

Another ASR system that may be possible to implement in the sandy ridge areas is The Freshmaker (Zuurbier et al., 2015). The Freshmaker is more suited towards shallow groundwater

systems that have salinity in the lower parts of the aquifer (Figure 4). This system utilizes two horizontally drilled wells. One deeper well extracts brackish water from the lowest part of the aquifer, to maintain the position of salt/fresh interface. The shallower horizontal well injects freshwater during times of surplus (wet season) and is also used to extract water during times of need (dry season). This system maintains freshwater extraction from the aquifer when it may otherwise be salty in dryer conditions.

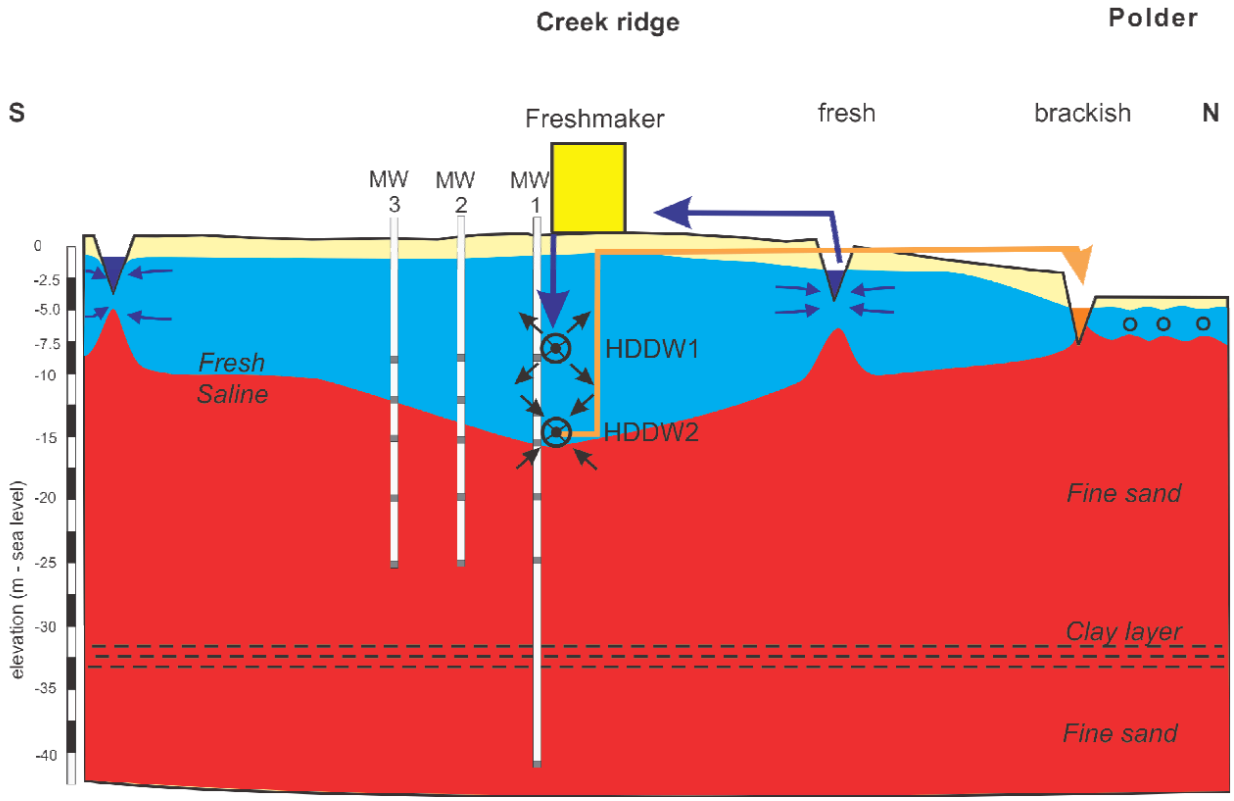

Figure 4 Cross section of a Freshmaker ASR system implemented on a creek ridge in The Netherlands, with two horizontally drilled wells (HDDW) and monitoring wells (MW) (Zuurbier et al., 2015).

Horizontal extraction wells can be utilized in both of these ASR systems. The implementation of horizontal wells is also worth considering as a water management technique in itself. When compared to vertical wells, horizontal extraction cause less drawdown and can reduce the upconing of seawater (Pauw et al., 2015).

In the context of ASR systems, the recovery efficiency (what fraction of the injected water is recovered) and storage capacity, are dependent upon the lithology, structure, thickness, depth and extent of the aquifer (Rambags et al., 2013). In order to assess the hydrogeological feasibility of an ASR system, the aquifer thickness, heterogeneity and bounding layers must be known. For example, a high potential sandy ridge aquifer in the MKD may consist of a homogenous sand layer, bound by aquitards, with adequate thickness to store water that can bridge the gap between water demand and supply.

1.3 Geologic context

The area of the Vietnamese Mekong Delta considered in this study is the lower sub-areal delta plain. The sediments in this area began deposition around 3ka when the coastal environment

shifted from one of tide-influence, to more wave influenced (Ta et al., 2002b). This area is characterized by well-developed rows of beach ridges with sometimes dunes on top that trend northeast to southwest. They can be 3m to 10m above mean sea level and are typically separated by interridge swamps or swales. The sandy ridges themselves are known to consist of well sorted, fine sand, making them suitable aquifers for ground water use (Ta et al., 2011). Many of the sandy ridges are currently being utilized for irrigation purposes. The sandy ridge structures in this area show promise as sites for potential implementation of ASR.

There are 953km^2 of relict beach ridges in the MKD (Figure 7)(Minderhoud, 2019). These structures appear as elevated features with sets of elongated branches on DEMs (Digital Elevation Models). The small branches usually stem from a larger trunk. The ridges are curved and generally run parallel to the coastline. In the Tra Vinh province, the width of these sandy ridges was found to be typically 1-2km with muddy inter-ridge swale deposits running in-between the beach ridges (Tamura et al., 2012). Figure 5 shows the branching sandy ridge structures of the Ben Tre and Tra Vinh provinces in the high-resolution DEMs.

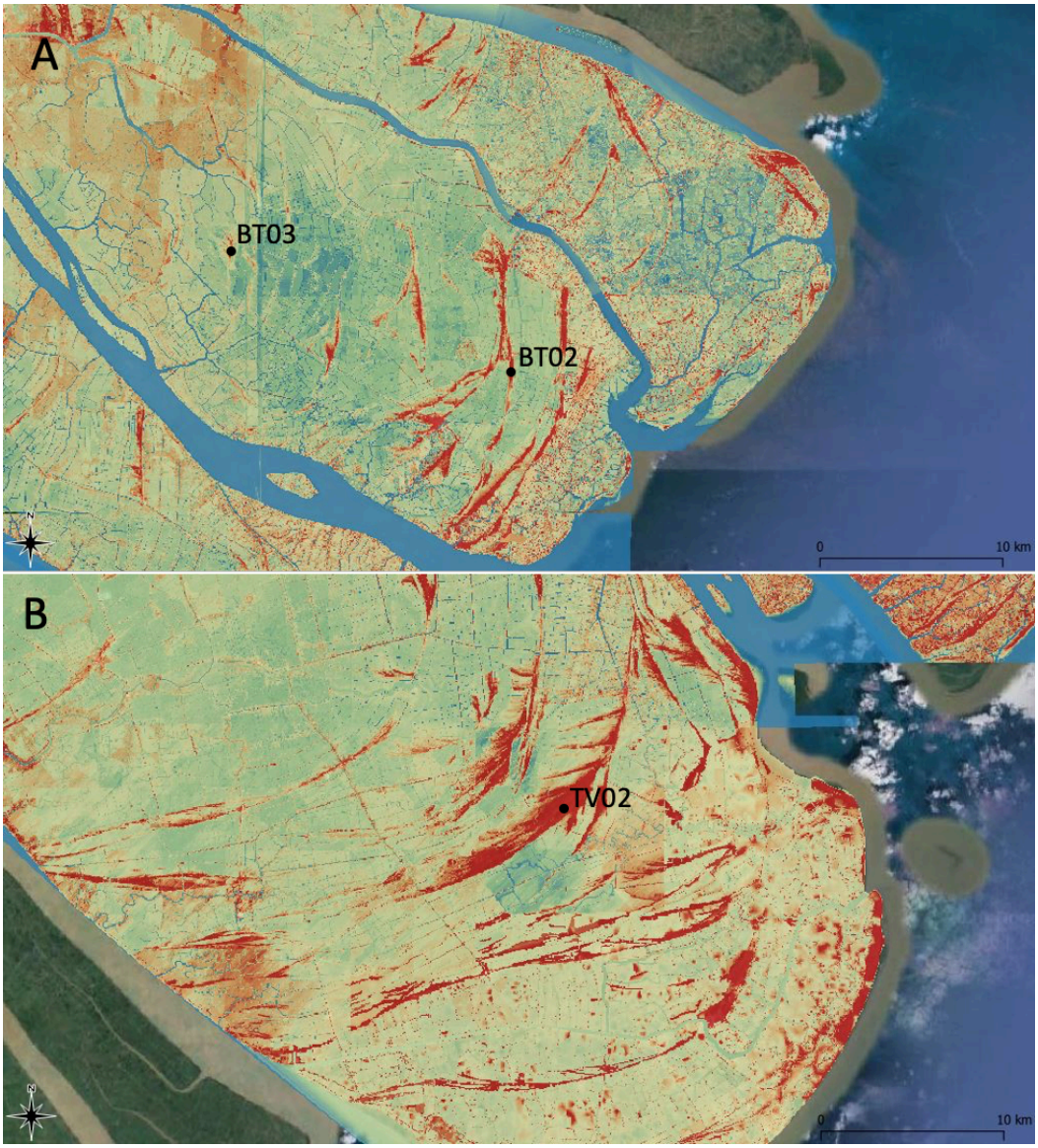

Figure 5 High resolution DEM showing sandy ridge structures in Ben Tre (A) and Tra Vinh (B), as well as the specific locations of the evaluated field sites in this study (BT03, BT02, TV02).

These ridges follow a distinct morphological pattern. They were formed during a progradation of the delta as sediment drifts along the shoreline from river discharge (Tamura et al., 2012) (Figure 6). The ridges begin as subaerially exposed islands and expand to longer spits of land as they accumulate sediment. The sub ridge sets are branches of the larger sandy ridge as sediment continues to accumulate and is influenced by wave tide and fluvial processes (Tamura et al., 2012). The ridges are very morphologically similar and follow the formation pattern depicted in Figure 6. The ridges can be identified in digital elevation models as they are distinctly higher than the other delta plain sediments and have a unique shape.

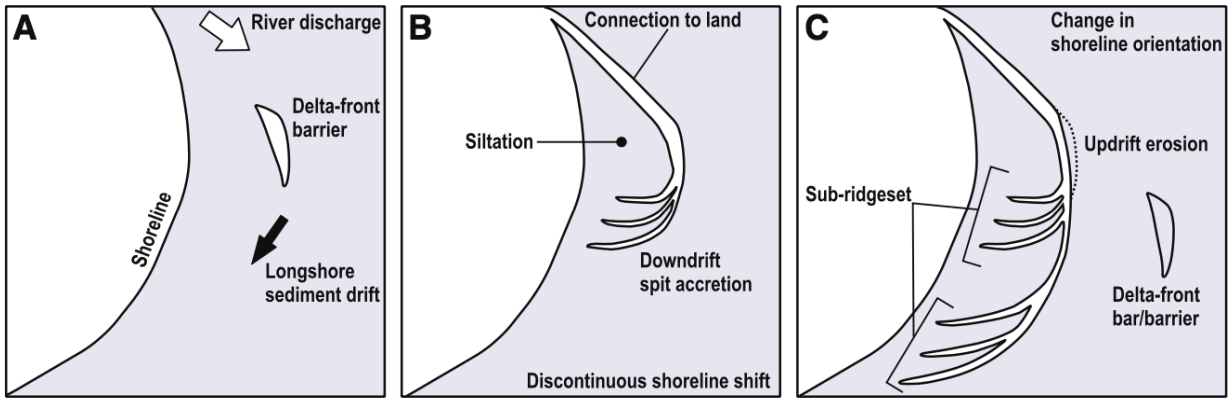

Figure 6 Depiction of Tra Vinh beach ridge development during progradation of the delta, including base ridge formation and sub-ridge sets (Tamura et al., 2012)

These structures are hydro-geologically significant because they differ from the typical upper Holocene Delta plain sediments. These uppermost sediments consist of silt, silty clay and clay (Minderhoud et al., 2017). This layer is largely considered to be an aquitard, having a high resistance to infiltration to fresh groundwater (Pham et al., 2019). The ridges present as sandy elevated features with greater infiltration capabilities than other surface deposits. During formation in the coastal landscape, the beach ridges/dunes are encompassed by low-energy depositional environments (Figure 7). The muddy inter-ridge deposits are significant as they may act as aquitards that isolate the shallow sandy ridge aquifers. This has control of the extent of the shallow aquifer. The thickness of the aquifer is dependent on the presence of aquitards that extend across the system. Coring reveals deeper older sediments that were deposited during earlier progradation stages of the delta (Figure 8). As these deposits become more coastal, then tidal, then marine with depth, it is probable that an aquitard will present itself binding the bottom of the system. For example a study of the Late Holocene progradation of the MKD by Ta et al. found that, in the Ben Tre province the prodelta mud deposits lie at approximately 15m depth from the surface (Ta et al., 2002a).

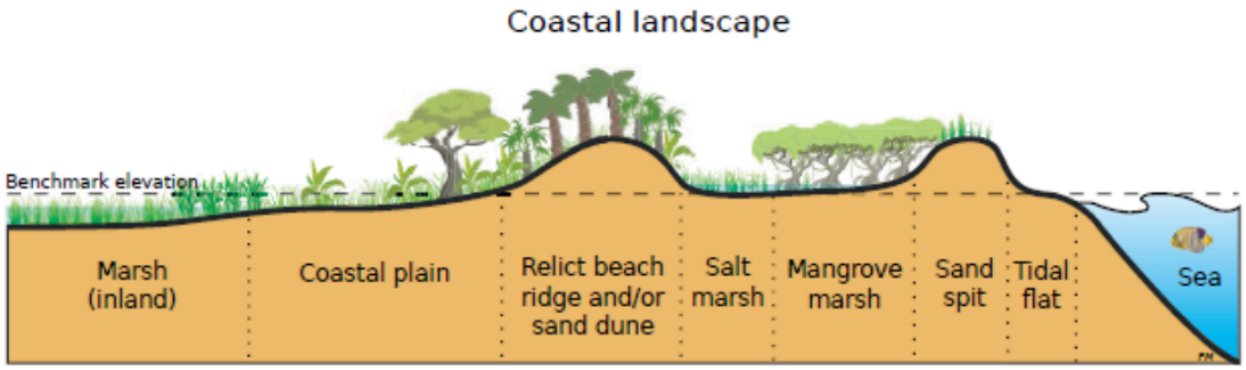

Figure 7 Profile of the delta coastal landscape showing relative elevations and depositional settings (Minderhoud et al., 2019)

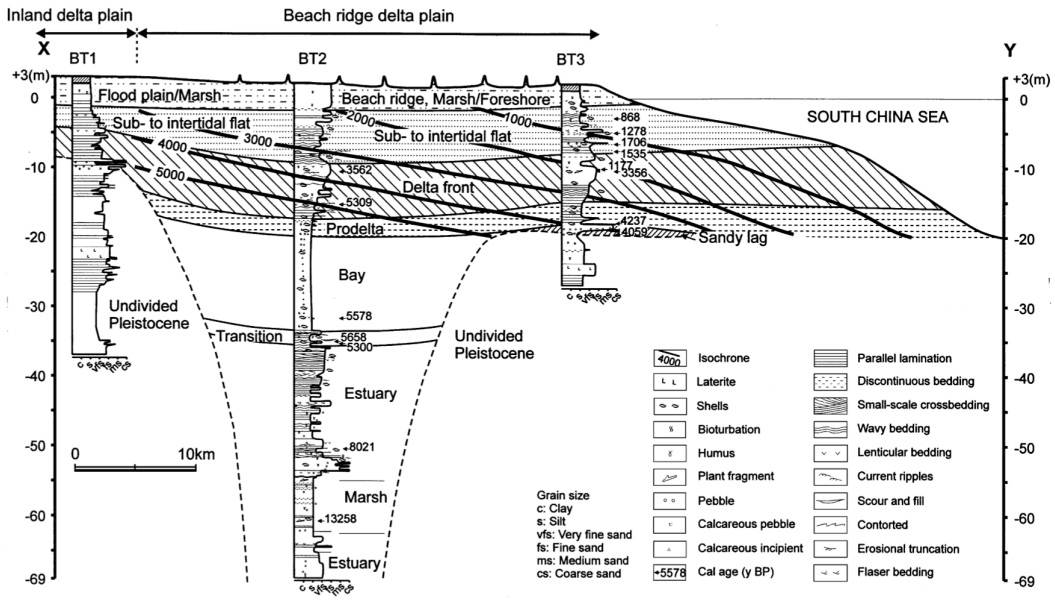

Figure 8 Cross section and core logs of sedimentary facies in the lower Mekong Delta plain the in the province of Ben Tre from (Ta et al., 2002a)

These aquifers may have the potential to benefit from aquifer storage and recovery techniques that have been implemented in the Netherlands in a similar delta environment. In order to implement water conservations projects, such as aquifer storage and recovery systems (ASR), suitability recommendations need to be made on a local scale. Establishing new knowledge about these sandy ridge systems is an early step towards the first pilot ASR system in the Vietnamese Mekong Delta. Water conservation projects, such as ASR systems, could be an important contribution to ensuring the survival of the delta's water supply.

1.5 Objective, research questions & approach

1.5.1 Objective

The objective of the research is to determine the architecture of shallow sandy ridge groundwater systems and assess their potential storage capacity. The data collected will be used to assess its potential for an aquifer storage and recovery system pilot. Part of this research involves developing a potential map of new shallow sandy ridge groundwater systems found in the MKD for further exploration.

1.5.2 Research Questions

The overarching research questions of this thesis is:

What is the hydrogeological potential of the shallow sandy ridge aquifers in the Vietnamese Mekong Delta for local aquifer storage and recovery solutions?

Sub research questions

To answer the overarching research question, three sub questions are considered. Questions I and II address the lithological and hydrogeological properties of the sandy ridges, and question III invites upscaling to new potential ASR sites.

I. What is the geological architecture of the sandy ridge aquifers found in the Tra Vinh and Ben Tre provinces?

II. What is the capacity for water storage in the shallow sandy ridge ground water systems?

III. What areas are most suitable for ASR solutions in the Tra Vinh and Ben Tre provinces?

Question I: Understanding the geologic composition, depth and thickness of layers within the aquifer is needed to estimate storage capacity and assess the suitability of the shallow aquifer. Presence of system boundaries, aquifer extent, depth and sediment suitability must be established to be able to estimate water storage capacity and its potential for expansion with an ASR system.

Question II: The storage capacity of the aquifer establishes the freshwater available for irrigation use. It also provides a way to estimate the available volume for infiltration from an ASR system.

Question III: The aquifer storage and recovery potential map and classification scheme made during this study will be useful to establish a way to identify additional shallow sandy ridge aquifers with the potential to benefit from an ASR system.

1.5.3 Research Approach

This MSc thesis is a part of the FAME (Fresh Water Availability in the Mekong delta) project, in association with Deltares, DWRPIS, WACC, Wageningen University and Research, Utrecht University, Nelen & Schuurmans and Royal HaskoningDHV. This project aims to increase the availability of fresh water, at a farmer scale, through the introduction of new water management techniques in the provinces of Ben Tre and Tra Vinh, in the Vietnamese Mekong Delta. In order to establish an ASR system, potential sites need to be evaluated to determine if the conditions are favorable. For this project, potential sites were selected at Deltares, based on criteria such as; construction suitability, existing data geology, surface water availability, farm size, urgency, land use and groundwater use. These sites are located on elevated sandy geomorphological features that showed promise for an ASR pilot system to be installed (Figure 5). The selected sites were evaluated in further detail by students, to select one for an ASR pilot. Two of these sites are in the province of Ben Tre (BT02 and BT03), and one site in the province of Tra Vinh (TV02). BT03 is in the middle of the Ben Tre province, and features; orchards and houses on top of sandy ridges, seasonal crops in the lower areas, water holes used for irrigation,

and subtle changes in elevation. BT02 is located further towards the coast in the Ben Tre province and features; the smallest sandy ridge of the three sites, many houses on top of the sandy ridge, and small rice, cattle and fruit farms. TV02 is located in the eastern part of the Tra Vinh province, and features; the largest sandy ridge studied, large fields with seasonal crops, scattered houses, and a surface reservoir built by the Adaptation in the Mekong Delta project (AMD). A team of three students that set out to evaluate these sites, and represent three components of this evaluation:

1. Agriculture, water use/demand, and irrigation. Sep Bregman, Wageningen University and Research, The Netherlands
2. Hydrology, water quality, and monitoring devices (piezometers, and rain gauges). Anne Kruijt, Utrecht University
3. Geologic architecture and aquifer storage capacity. Josh Shankel, Utrecht University.

This MSc thesis focuses on the 3rd component, concerning the lithological makeup of the sandy ridge aquifers and the volume of groundwater that can potentially be stored, as well as the locating of new sites for exploration. All three studies are useful in making recommendations that will further the research of the FAME project on these sites. The data and analysis used for this thesis is designed to be considered together with the other two components for the purposes of the FAME project. This will provide a comprehensive assessment for further research and evaluations.

The hydrogeological potential of ASR for the sandy ridges in Mekong Delta will be answered by addressing the three sub research questions of this thesis. Sub research question 1 is answered by utilizing deep coring and shallow suction coring to create lithological cross sections. The visualization of the subsurface will reveal the architecture of the sandy ridge structures, which can then be evaluated based on characteristics that are suitable for ASR. Sub research question 2 is answered by utilizing the lithological characteristics obtained from the cross sections as well as groundwater level data, to estimate the volume of water that can be held in the pore spaces within the sandy ridges. This will be possible by utilizing a customized program in MATLAB. The shallow geological architecture is required to be able to reasonably estimate the storage capacity, understand how the subsurface systems function and assess if the conditions are suitable for storage. A potential ASR system needs favourable subsurface conditions to make implementation feasible. The idealized aquifer for an ASR system is unconfined, homogeneous (with no obstructing low permeability layers), has aquitards binding the system, is composed of sandy sediments, and has large storage capacity. The closer the aquifer is to these conditions, the more favourable the site is for an ASR system. The storage capacity will be estimated at three levels; the surface to groundwater level, the groundwater level to the lowest yearly groundwater level and the estimated volume of the entire sandy ridge. Sub research question 3 is answered by utilizing mapping data to find sandy ridges that show potential to benefit from ASR. The utilized data will come from surface water saltwater intrusion data from 2016, a land cover classification map and a digital elevation model.

3 Methods

3.1 Field methods

3.1.1 Coring site selection

Three research sites (TV02, BT03 and BT02) were selected previously based upon suitability field trips for an ASR pilot. The initial phase of study begins with selecting locations in which to explore the subsurface with shallow suction coring devices. These locations were selected by exploring digital elevation models (DEMs), using GIS software. The DEMs are based on LiDAR data with a 5m resolution. Using the DEM gives a more objective view of the position of the sandy ridge. Preliminary coring site selection was used to observe where potential cross sections can be made perpendicular to the sandy ridges. The more linear these cross sections are, the higher resolution the subsurface architecture will be for analysis and interpretation of layers. The coring sites were selected away from buildings and infrastructure, and closer to large trees and undisturbed land, when possible, to get a more accurate representation of the natural state of the sandy ridge. This also diminishes the influence of wells on groundwater level data. Ideal coring sites for cross sectional purposes were often obstructed by buildings and fences.

3.1.2 Coring protocol & strategy

Sites were selected that would cover corings over two sandy ridges in the area of the BT03 site and TV02, in a linear fashion, with regular intervals when possible. Additional coring sites, that were off the sandy ridge area, were chosen for additional exploration of the geology of the system, and hydraulic gradient relative to a water source (ditch). It should be noted that a different approach was taken for the BT02 site. Three smaller cross sections, instead of one were created to explore the consistency of the sandy ridge structure.

A hand auger and two Van der Staay suction coring devices were used to extract the sediment for logging. An Edelman auger (a hand operated tool used to remove sediments in 10cm increments) was used to extract the sediment above the saturated zone. When the water table is reached a water level measuring tape with sensor was lowered into the bore hole, and the current ground water level was recorded. The Van der Staay coring devices were then used to extract the sediments below the water table (Figure 9). The sediment can then be analyzed and logged in 10cm increments. More detailed protocol is available in the Appendix A.
Due to the nature of the sediment and available materials, it was only possible to core to a maximum depth of 4m. For this, a 2m and a 4m Van der Staay were used. In the event of a clay layer, a gauge was used to core past it. In order to reach the base of the shallow aquifer system a local drilling team was used that could core down at least 10m. Finding the clay base of the system was necessary for estimating storage capacity. Deeper cores (past 4m) were completed with and automated drilling rig. All the deeper cores at the BT03 site were logged in detail. Exact depths are less reliable with deeper coring as approximately 75% of the core is recovered.

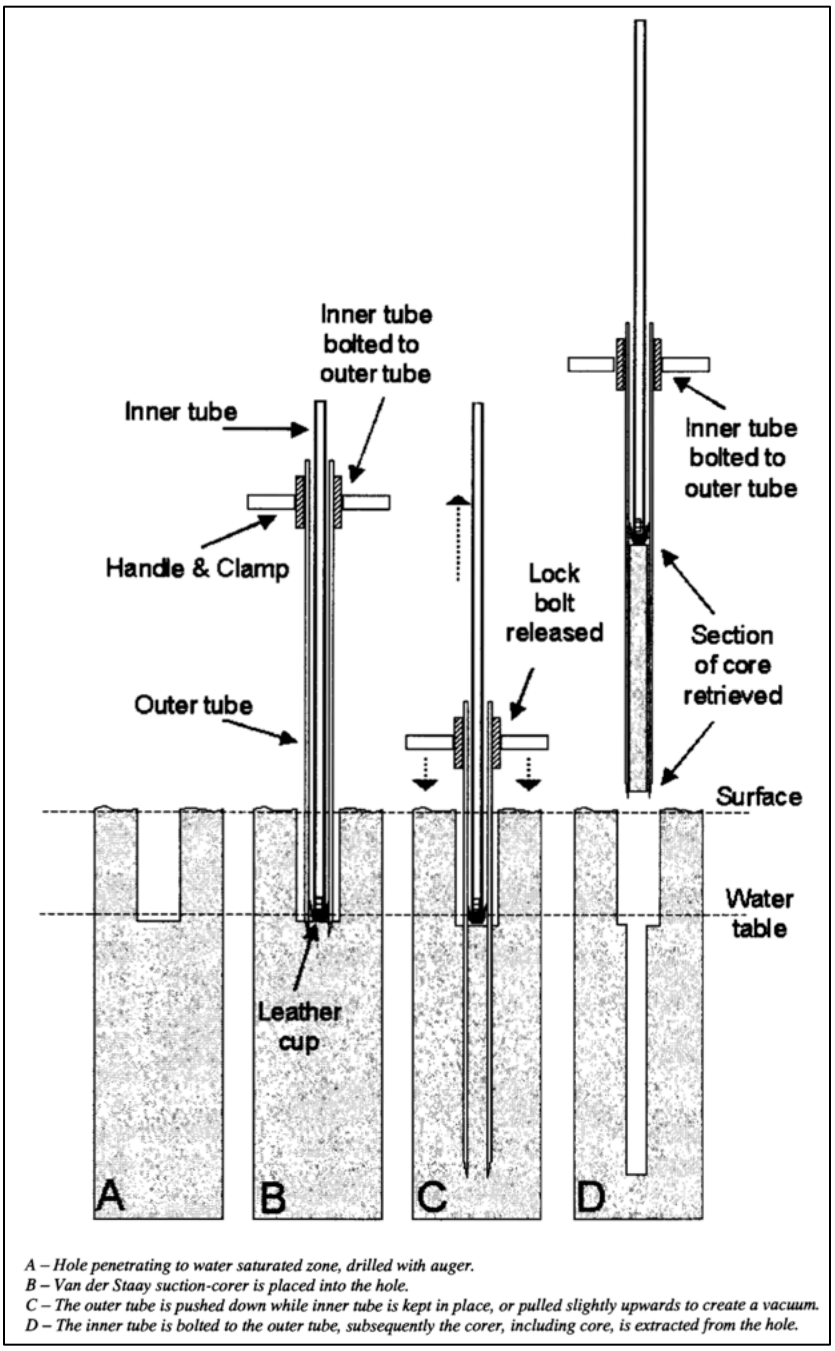

Figure 9: Depiction of working principles of the van der Staay suction coring apparatus (Wallinga and van der Staay, 1999)

3.1.3 Logging

The sedimentary observations during the logging process were used to observe water level fluctuations and to understand lithology. The coring data is used for analysis of sandy ridge architecture, geologic settings, water level changes, and hydrogeologic horizons used for storage capacity calculations. The primary focus of this logging focuses on: grain size, texture, sorting, groundwater levels and reduction/oxidation zone boundaries. More information was also collected concerning: fossils, organic matter, plant remains, calcium carbonate, and any other notable features. Observations were recorded on bore log sheets in the field for every 10cm of

core. Positions of cores were recorded using a GPS using the UTM positioning system. More reliable elevation data was obtained by plotting the coring sites on the DEM in GIS. Grainsize was measured using a sand ruler, texture was classified by using a USDA soil texture classification triangle, and the reduction zone boundary depths were observed clearly due to high concentrations of oxidized iron in the sediment. The reddish/brownish oxidised sands show that the sediment has been exposed to air, while the black and greyish sands show that the sediment lies below the lowest water table level. This is known as a redoximorphic feature, and is evidence of the oxidation of iron from Fe(II) to Fe(III) in the following reaction.

$$O_2 + 4\mathrm{Fe}^{2+} + 4H^+ \rightarrow 4Fe^{3+} + 2H_2O$$

This reaction can occur within 30 minutes of the sediment being exposed to the air (Vepraskas, 1992). On the sites studied, this is was a reliable way to determine the groundwater levels at the maximum level of depletion during the dry season. This provides a reference point for the level of head depletion. The sediments present in these areas of the Mekong Delta have a high degree of iron content and show distinct, an easily observable boundary (Figure 10). Samples were also taken from the cores for further analysis in the lab, in order to obtain grain size distribution curves to estimate effective porosity and clay fraction. Unfortunately, the lab was unavailable to process these samples. Porosity values from literature were used as a substitute.

Figure 10 Section of core featuring a redoximorphic feature.

3.2 Cross section Analysis

To establish lithological interpretation, hydrogeological horizons and estimate storage capacity it was necessary to create two different cross section types. The preliminary analysis uses the LLG software (a core logging software that maps and displays cores and creates cross sections) provided by the university. This was useful for observing correlations in the field and interpreting lithological horizons. To estimate storage capacity and display hydrogeological horizon lines, a core processing program was established, that uses MATLAB.

3.2.1 MATLAB

A MATLAB program, that was developed by a fellow peer Stan Schouten at Utrecht University, is able to display the cross sections and allows for the input of horizon lines. This software is also capable of calculating the area between created horizons by integrating between two lines. This tool was used to calculate the area between the surface and the base of the sandy ridge as well as the areas occupied between the surface, current groundwater level and lowest groundwater level. This method doesn't allow for calculation of horizons that are not continuous across the entire cross section. Instead of classifying horizons based on the sediments, a range of effective porosities were used to get a minimum and maximum storage capacity. This was possible due to the fairly homogenous nature of the systems. Utilizing a range of effective porosity values was more viable for this data set due to the uncertainty from extrapolating horizon lines and upscaling. The minimum effective porosity was assumed to be 0.25, which has been used to model a both sand and clay layers in the Vietnamese Mekong Delta in (Pham et al., 2019). This value used to represent typical effective porosity in this area of the Delta. An effective porosity value of 0.30 was used on the higher end, to reflect the higher degree of sand present in the sandy ridge areas. This value is commonly used in modeling sandy aquifers, and was used by (Pauw et al., 2015) when modeling similar sandy aquifers in the Netherlands.

3.3 Upscaling

The intent of the upscaling is to be able to estimate the storage capacity of the sandy ridge aquifer across the estimated length of the sandy ridge. To assess the sandy ridge aquifers a suitability regime was created to give a rating to studied sites so they can be easily compared and referenced to an ideal aquifer. This is based on the hydrogeological characteristics detailed in this section. This was applied to the study sites visited during the field campaign. For further research an ASR potential map was established to explore new potential field sites.

3.3.1 Storage Capacity

The storage capacity was first calculated in 2D. This, per stretched meter, value was then multiplied across the length of the estimated sandy ridge system. The storage capacity of the sites is calculated by calculating the areas between horizon lines, and then stretching that area across the system to get to a storage volume. For example, the BT03 sandy ridge is approximately 1km long and the storage capacity was calculated along this length. The storage volumes between the horizons are calculated as well as storage for the entire cross-sectional area. The horizons include the base of the system (aquitard), the lowest groundwater level, the observed groundwater level, and the surface. The surface level to groundwater level storage capacity is assumed to be the volume available for fresh water infiltration at the time of the field campaign (at the start of the dry season, when surface waters are still fresh). There is a maximum and minimum storage capacity based on effective porosity estimations (0.25-0.3). The maximum assumes there is 100% fine sand in the cross-sectional areas, and the minimum assumes a mix of sand, clay and loam, that is more typical for other areas of the delta. The void volume was calculated using effective porosity to give a value that represents water residing in connected pore spaces, that is usable for extraction. The volume of voids was calculated by the porosity formula (Fetter, 2018). Where n_e is the effective porosity, V_v is the volume of the void space and V_T is the total volume of the sediment.

$$n_e = \frac{V_v}{V_T}$$

The storage volume was first taken as per stretched m (calculated in 2D), and then stretched across the length of the system observed in the DEM. This allows for the estimation of storage capacity for the agricultural community that utilizes the sandy ridge aquifer system.

3.3.2 Site Suitability

A site suitability scoring system was developed based on a methodology used for creating suitability maps in the Netherlands for creek ridge infiltration ASR systems. This system is loosely based on creek ridge infiltration parameters created with modeling and field experiments in a study by (Pauw et al., 2015) and the tables 1 and 2 are inspired by (Delsman et al., 2015). The combined hydrogeological and geological factors are what determine the site suitability of this type of ASR system. The system has been adapted for the available hydrogeological data from this study. This scoring technique can be applied to the shallow sandy ridge aquifers in the Mekong Delta when selecting new sites after similar data has been gathered. The factors and scoring for suitability are shown in Table 1. Table 2 shows the suitability classifications created through evaluating the combination of these scores. Factor A is determined with DEMs using GIS, where elevated elongated sandy ridge structures are present in rural areas, often running parallel to the coastline. Factor B, C, D, & E are determined by geological exploration through coring and the cross-section interpretations. The purpose of factor D is to identify potential layers with high clay content that could inhibit groundwater flow and / or infiltration. Factor F is determined by the storage capacity calculation and the estimated space available upwards from the groundwater levels present at time of field campaign (Late October – mid December) at the end of the wet season and beginning transition into the dry season. To enlarge the freshwater lenses, while preventing flooding, there should be at least 0.85 m of unsaturated sediment above the water table (Sommeijer, 2012). This system provides a simplified overview of the suitability of the sites, so that they can be easily compared with each other.

Table 1 suitability factors for sandy ridge infiltration suitability (*inspired and adapted from* Delsman et al., 2015)

	Criteria	Score	Criteria	Score
Factor A	Presence of elevated sandy geomorphological feature	1	absent	0
Factor B	Unconfined aquifer	1	Confining layers	0
Factor C	Significantly comprised of homogenous sand	1	Highly variable composition	0
Factor D	Absence of extensional low flow layers within target aquifer	1	Presence of extensional low flow layers	0
Factor E	Presence of horizontal and vertical aquifer boundaries	1	Absent or unknown	0
Factor F	Storage Capacity available during the end wet season with at least 0.85m of unsaturated zone).	1	rest	0

Table 2 Scoring to determine site potential for ASR system.

Suitability / potential	Score
Ideal	If A = 1 & B = 1 & C = 1 & D + E + F = 3
Good	If A = 1 & C = 1 & D + E + F = 1 or 2
Low / possible	If A = 1 & B = 1 & C = 1, D + E + F = 0
Not suitable	If A = 0 or C = 0 or B = 0

3.3.3 Potential Map for ASR

The purpose of the potential map is to identify sandy ridge/beach ridge structures that have the potential to be utilized for ASR systems. The potential map was created using the high-resolution LiDAR DEMs from the two provinces (5m resolution), an official land use map derived from Landsat 5 data from 2009 (30m resolution) (Minderhoud et al., 2018) , and a map of surface water salinity data in g TDS/L from the 2016 dry season (2km resolution) (Eslami et al., in preparation). The salinity map represents median salinity between January and April. QGIS software was used to create boolean raster layers that are multiplied with each other to yield sandy ridge areas that have high potential to benefit from an ASR system.
An ASR system would be used to provide water security and increase availability in the dry season. For this reason, the areas, in the land use map, areas that are cropping in the dry season or have orchards that grow all year were considered. These areas are more likely to be vulnerable to water shortages or saline intrusions in the dry season and will therefore benefit the most from such a system. The land use map isolates the areas that are assumed to irrigate using groundwater in these types of cropping schemes. Areas of aquaculture, and areas that crop less frequently are not considered a priority. These areas are reclassified into a boolean map that is used to identify areas that are at risk for lower dry season water availability (Figure 11)

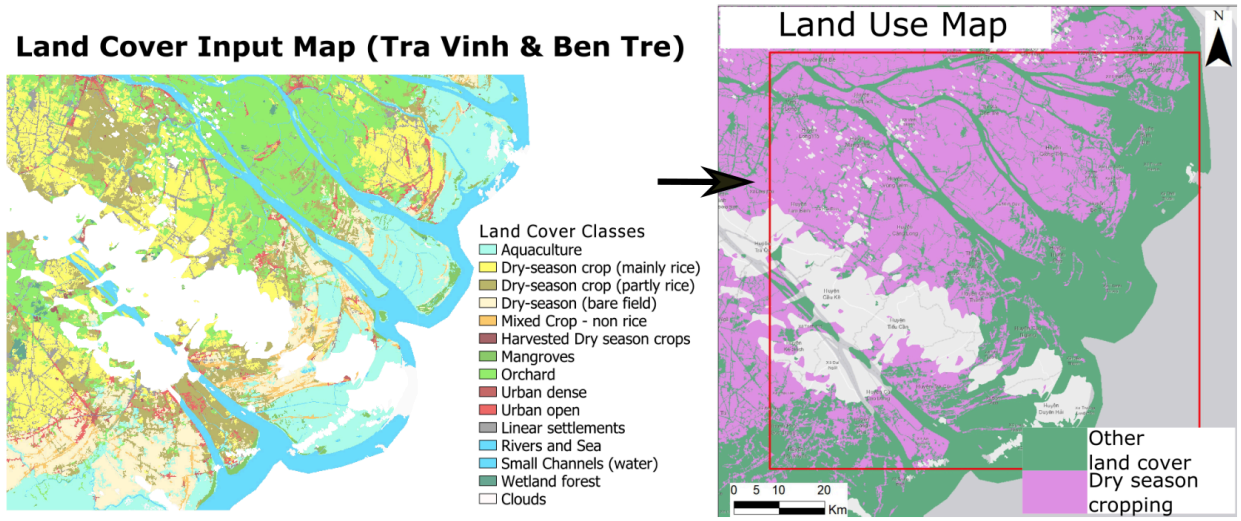

Figure 11 Land use input map based on 2009 Landsat data and reclassified boolean map for dry season cropping.

The salinity map is representative of an extreme year (2016) of record salinity intrusion, and drought following the El Niño of 2015-2016 (Eslami et al., 2019). Using this data, enables the identification of areas that are at risk during unusual climate conditions, and that can potentially be protected from such events. The salinity map shows areas that experience salt water intrusions in the surface water ways. Table 3 shows the classifications used to identify the severity of salinization, based on the usability of the salt contaminated water (Mayer et al., 2005). A cutoff of above 2 g/L of salinity (as that is considered the cutoff where the water becomes unusable for crops) was used to create a boolean map that shows the areas that are at high risk for surface water intrusion. The salinity map identifies areas that had high salinity surface water intrusions in 2016 (>10 TDS g/L), as well as areas that are classified marginal to saline (0.5 – 10 TDS g/L), and always fresh zones (<0.5 TDS g/L). Areas that are less affected or always have fresh surface water and areas that are deemed too saline are shown in a reclassification map used define areas

where ASR is; less possible (high salinity), high benefit (marginal – saline) and possible (always fresh zones), see Figure 12.

Table 3 Salinity classification and usability (Mayer et al., 2005)

Salinity status	Salinity (milligrams of salt per litre)	Description and use
Fresh	< 500	Drinking and all irrigation
Marginal	500 –1 000	Most irrigation, adverse effects on ecosystems become apparent
Brackish	1 000 – 2 000	Irrigation certain crops only; useful for most stock
Saline	2 000 – 10 000	Useful for most livestock
Highly saline	10 000–35 000	Very saline groundwater, limited use for certain livestock
Brine	>35 000	Seawater; some mining and industrial uses exist

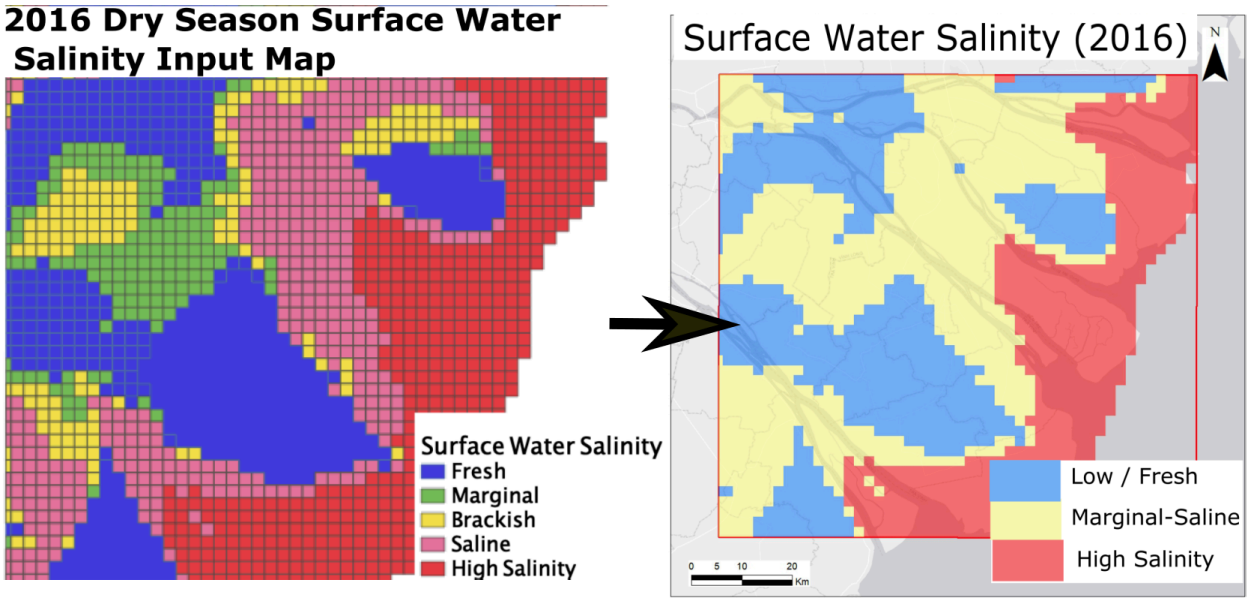

Figure 12 Surface water salinity input map and resulting map for ASR salinity classifications.

The DEMs of these areas isolate elevated features above 1.5m above MSL. This is used to pick out the higher elevation sandy ridges. This height was chosen as all sandy ridges studied have an elevation of at least 1.5m, so this cutoff enables the identification of similar structures (Figure 13).

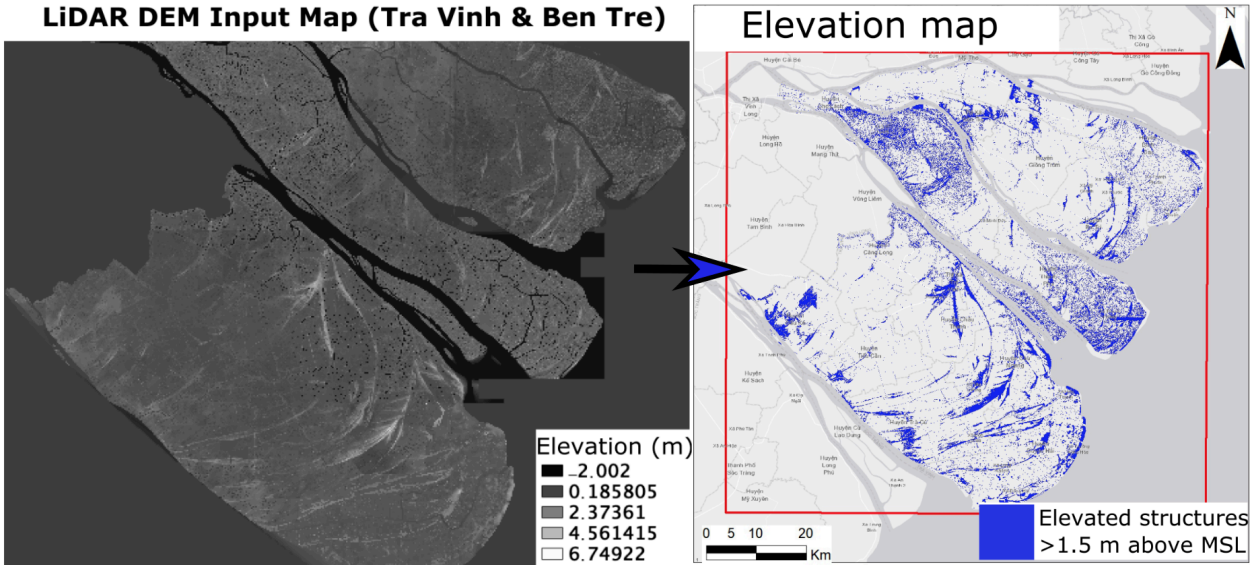

Figure 13 High resolution LiDAR DEM of Ben Tre and Tra Vinh input map and resulting boolean map isolating elevated structures.

By making boolean maps these three factors allows the visualization of shallow sandy ridge aquifers (above 1.5m) in the Tra Vinh and Ben Tre provinces that use groundwater in the dry season and are at higher risk for salt water intrusions. These maps are multiplied together to produce Figure 25. The DEM of the elevated areas is converted into a vector layer, so that the shape and area of the total sandy ridge structures can more accurately be identified. This way, the sandy ridges in the suitable areas can be identified from morphology and separated from built up areas, and issues with reduced resolution from combining multiple maps can be accounted for. This map is overlain on the resulting boolean map to add sandy ridges back in that intersect with the boolean map. Built up areas and areas that are not morphologically similar to sandy ridge structures that were included in the DEM map are manually eliminated. The sandy ridges in fresh water areas and sandy ridges covered by clouds in the land use map are also manually picked out of the vector layer and added into the ASR potential map.

4 Results

4.1 Sandy ridge Architecture

An overview map of the sites is provided in Figure 5, and close up maps of the specific sandy ridges and cores are displayed in this section. This section is organized by presenting results and observations for each site individually. The Ben Tre 03 (BT03) site covers two sandy ridge structures, the Ben Tre 02 (BT02) site covers the smallest sandy ridge with three cross sections, and the Tra Vinh 02 (TV02) site shows the largest sandy ridge structures studied.

4.1.2 Ridge Architecture of Ben Tre field site BT03

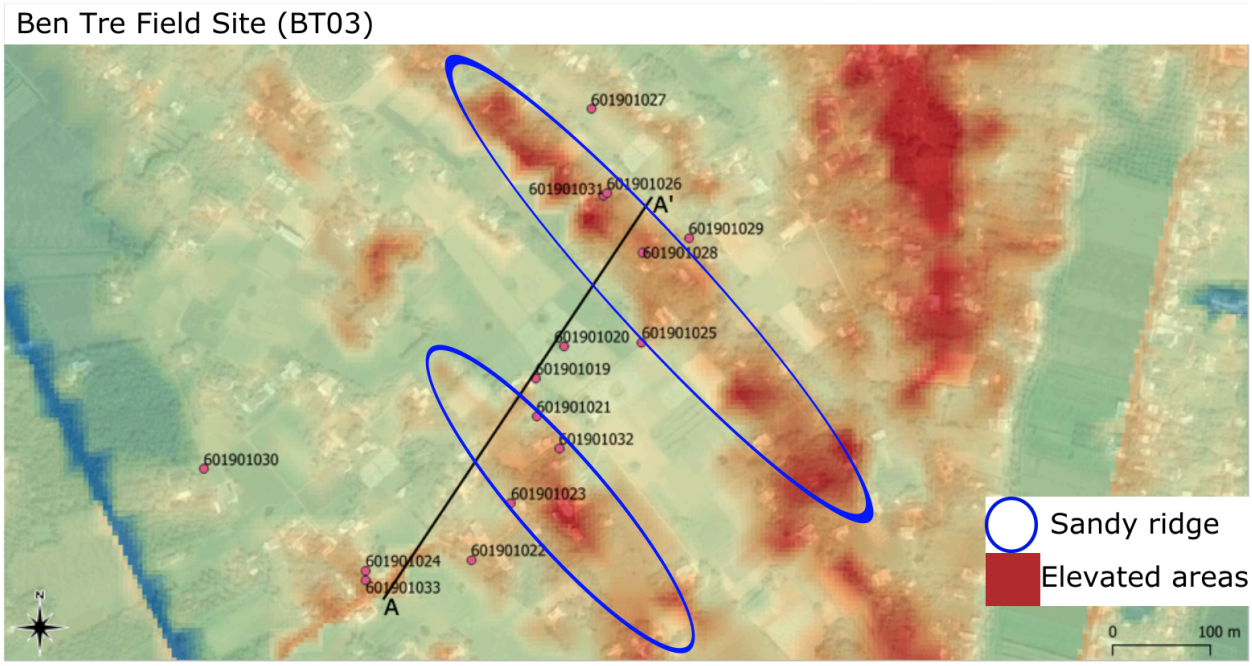

Figure 14 LiDAR elevation map depicting the two sandy ridge structures of the BT03 site, with coring sites and cross section line.

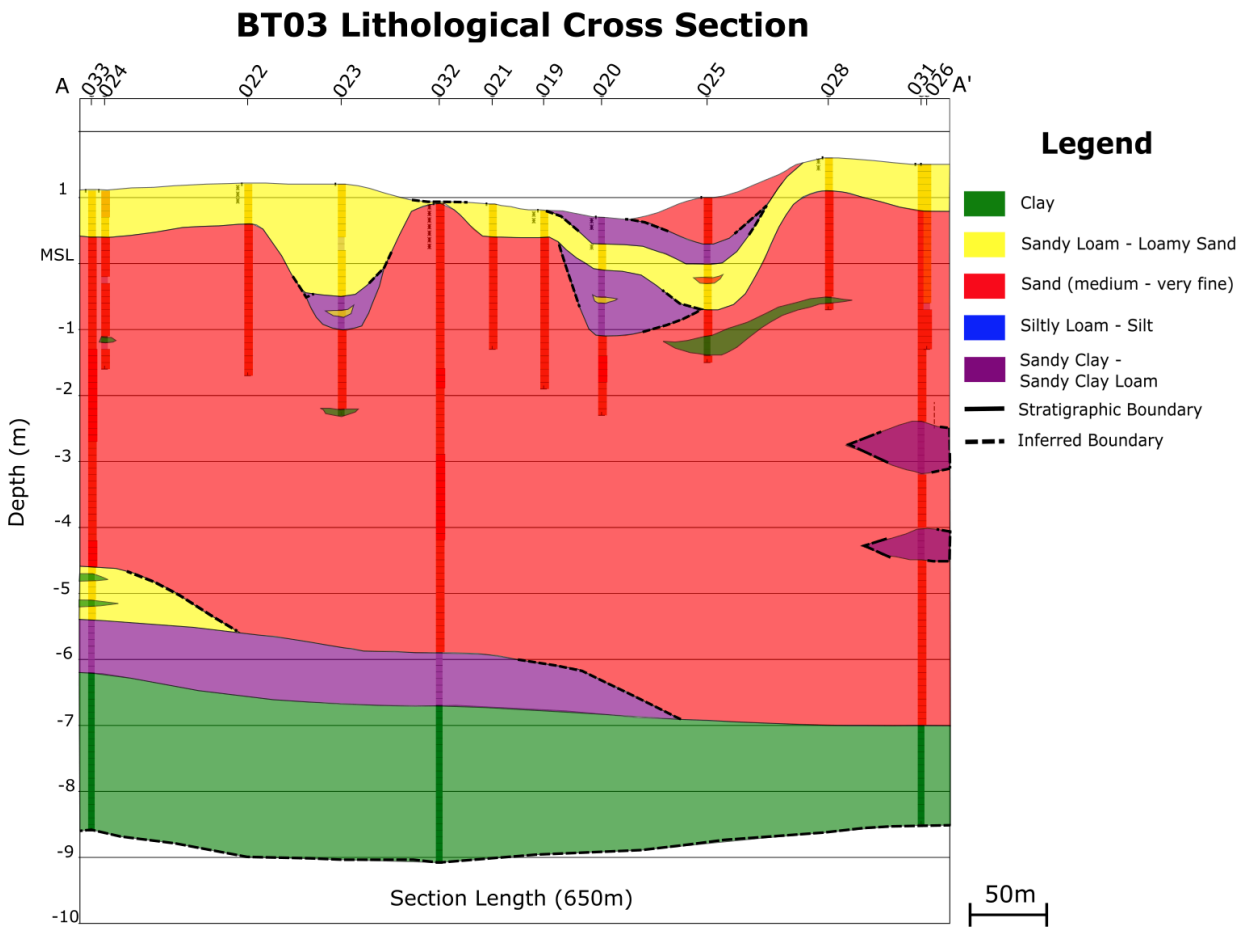

Figure 15 Ben Tre site BT03 lithological cross section depicting subsurface interpretation of architecture, sediment types and boundaries, created using the LLG software.

The BT03 (Ben Tre 03) site covers two sandy ridges over a span of approximately 600m. The upper 1-2m consist mainly of layers of sandy clay (SC), sandy clay loam (SCL) and very fine sand (Vfs). This top most layer is very likely to have a high anthropogenic influence. There is a thick clay layer present approximately 6.5 meters below MSL that continues for the duration of the cross section. This is considered to be the "base" of the system and a system boundary, assumed to be an aquitard. This clay layer is only observed by the three deeper cores and is assumed to be present throughout the system. Recovery of the deeper cores is approximately 75%, so the exact depths are less reliable than the shorter cores. The majority of the aquifer consists of fine sand (fs) with some areas of (Vfs) and medium sand (Ms). There are a few thin clay layers present in the aquifer. They have a maximum thickness of 30cm and appear to be discontinuous. The sand layer from the surface is approximately 7.5m thick. This site is represented of the pinnacle of the field methodology development and has the highest degree of confidence, compared to the other sites.

4.1.3 Ridge Architecture of Ben Tre field site BT02

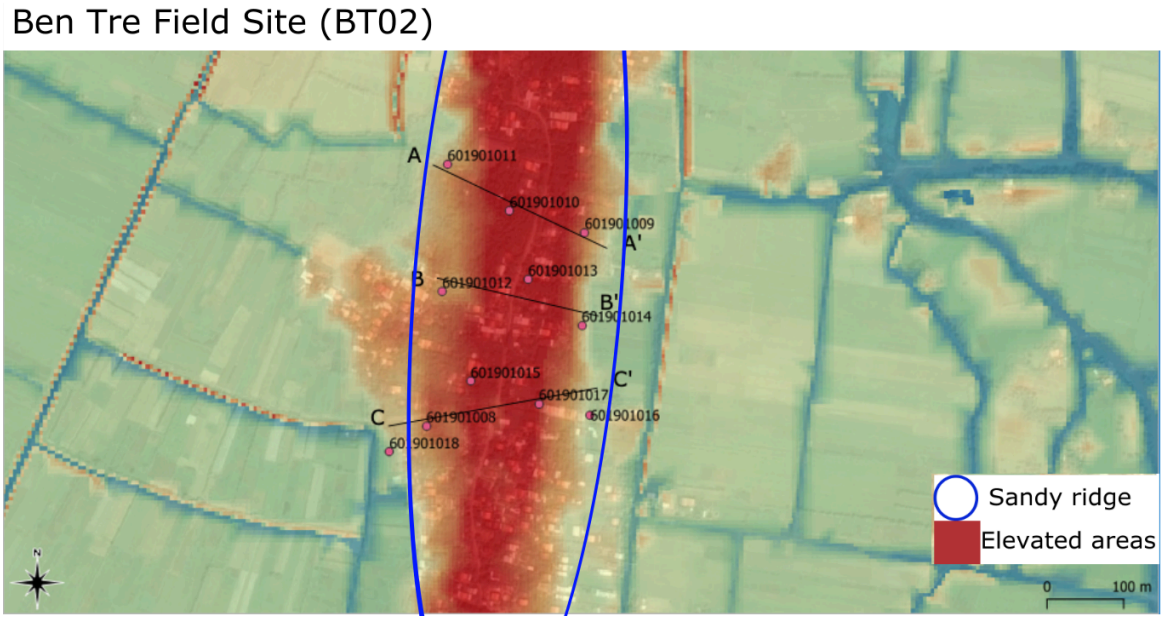

Figure 16 Elevation map depicting the small sandy ridge structure of the BT02 site, with coring sites and cross section lines A,B & C. Note: Cores 17 and 34 are in the same location.

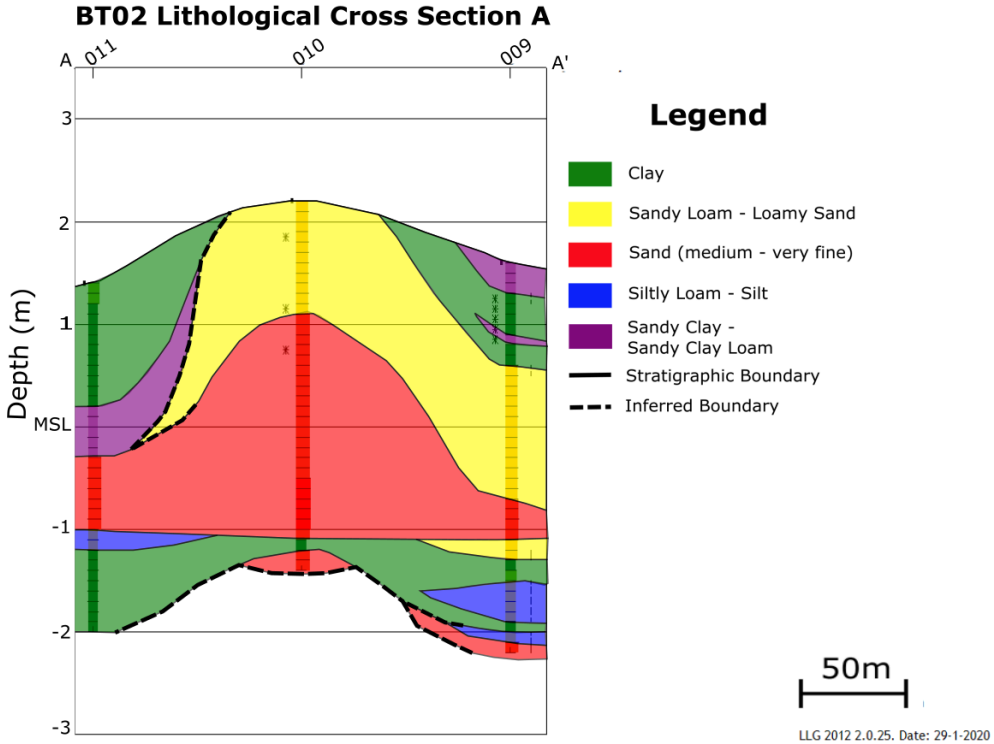

Figure 17 Cross section 1 depicting subsurface interpretation of architecture, sediment types and boundaries, created using the LLG software

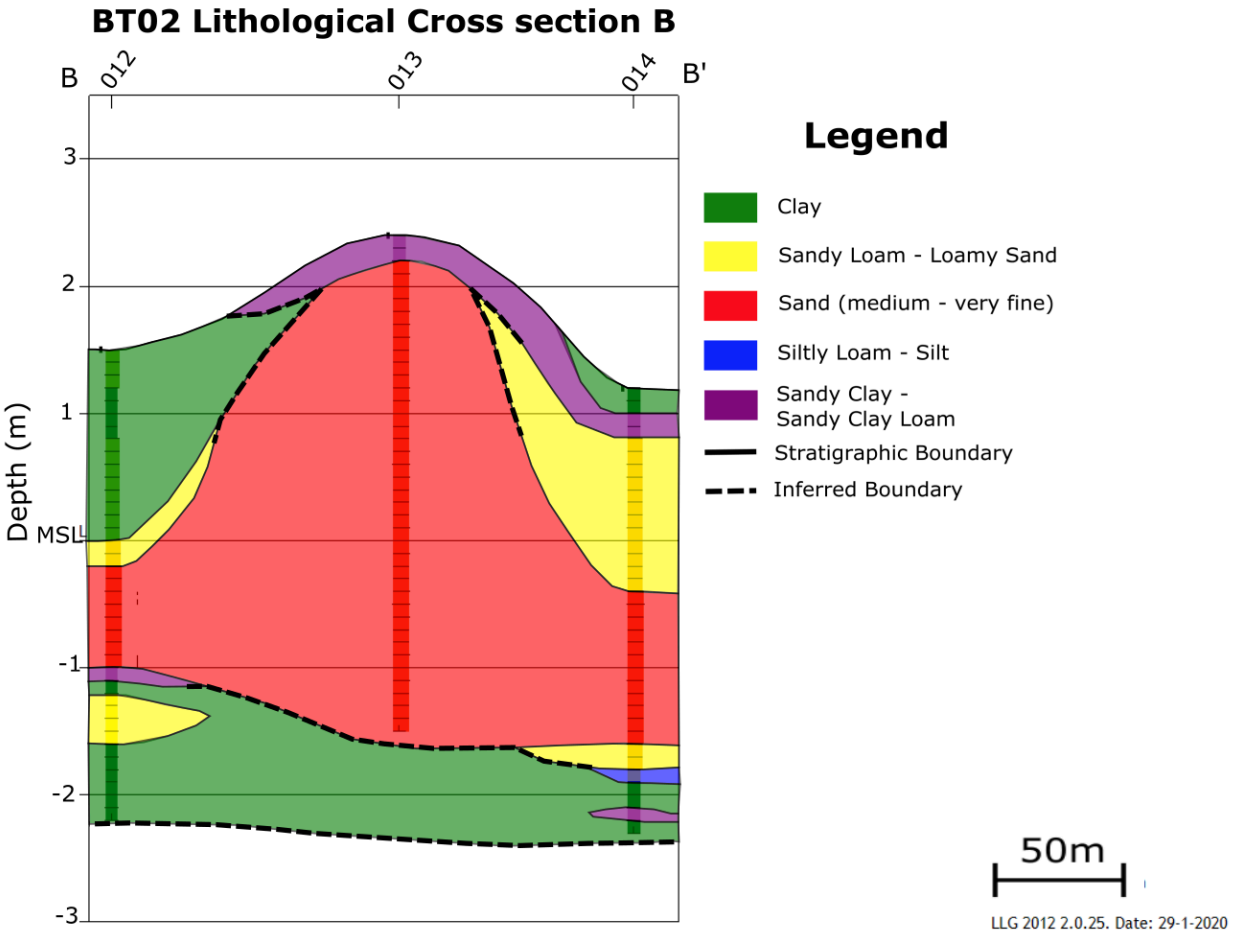

Figure 18 Cross section 2 depicting subsurface interpretation of architecture, sediment types and boundaries, created using the LLG software.

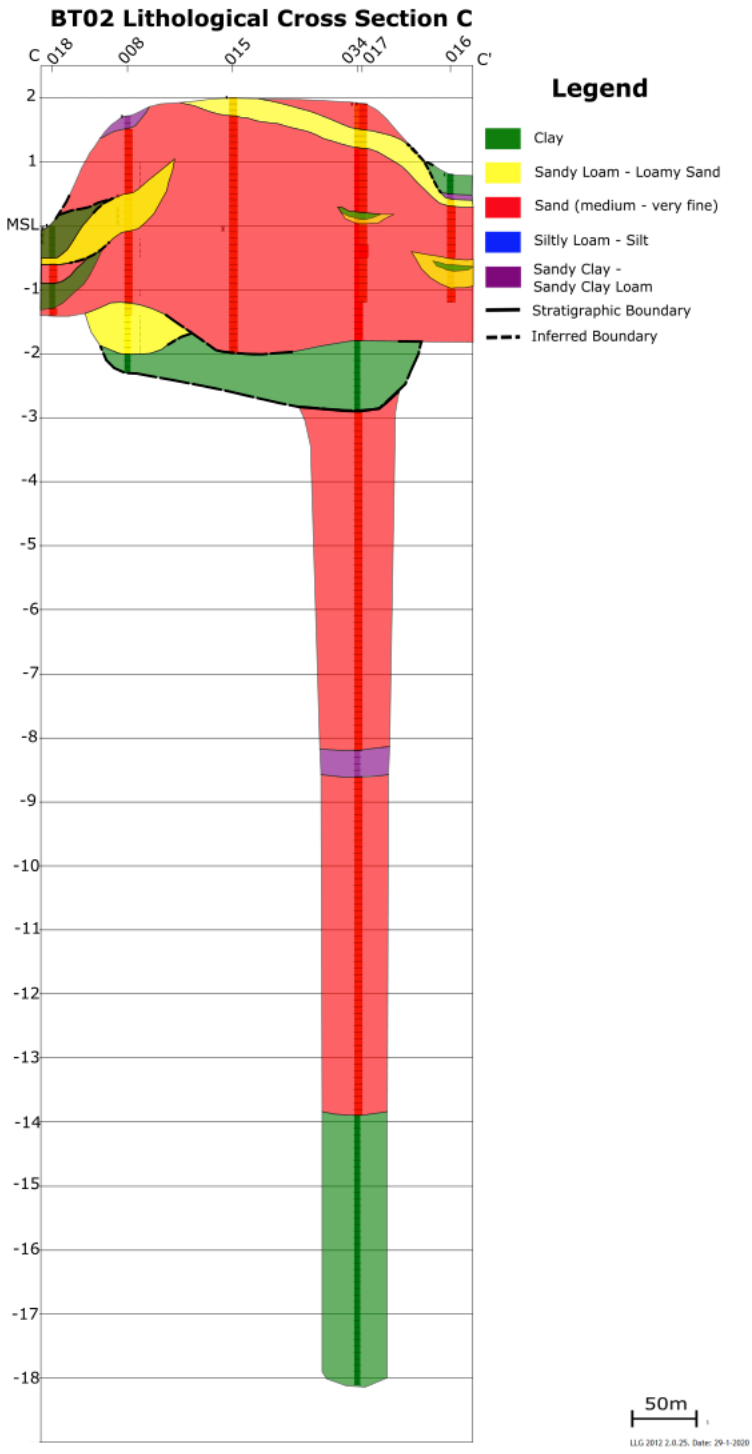

Figure 19 Cross section 3 depicting subsurface interpretation of architecture, sediment types and boundaries, created using the LLG software.

The sandy ridge is much smaller than the other sites, being only approximately 200m wide, and there were many buildings and roads obstructing potential coring locations. The top 1.5m of depth, have a high degree of anthropogenic influence in on this site. In cores 12 and 15 there was plastic and glass found in the core within the first 1.5m, meaning that this layer is not

representative of the natural environment, making geological interpretations unreliable. There is a sand (Fs-VFs) layer that is at least 3m thick, that is consistent along all 3 cross sections. There are intermittent loamy sand layers (LS) on top and in-between the sand layers. There are also sandy clay (SC) deposits on the edges of cross section 1(Figure 17), and on top of cross section 2 (

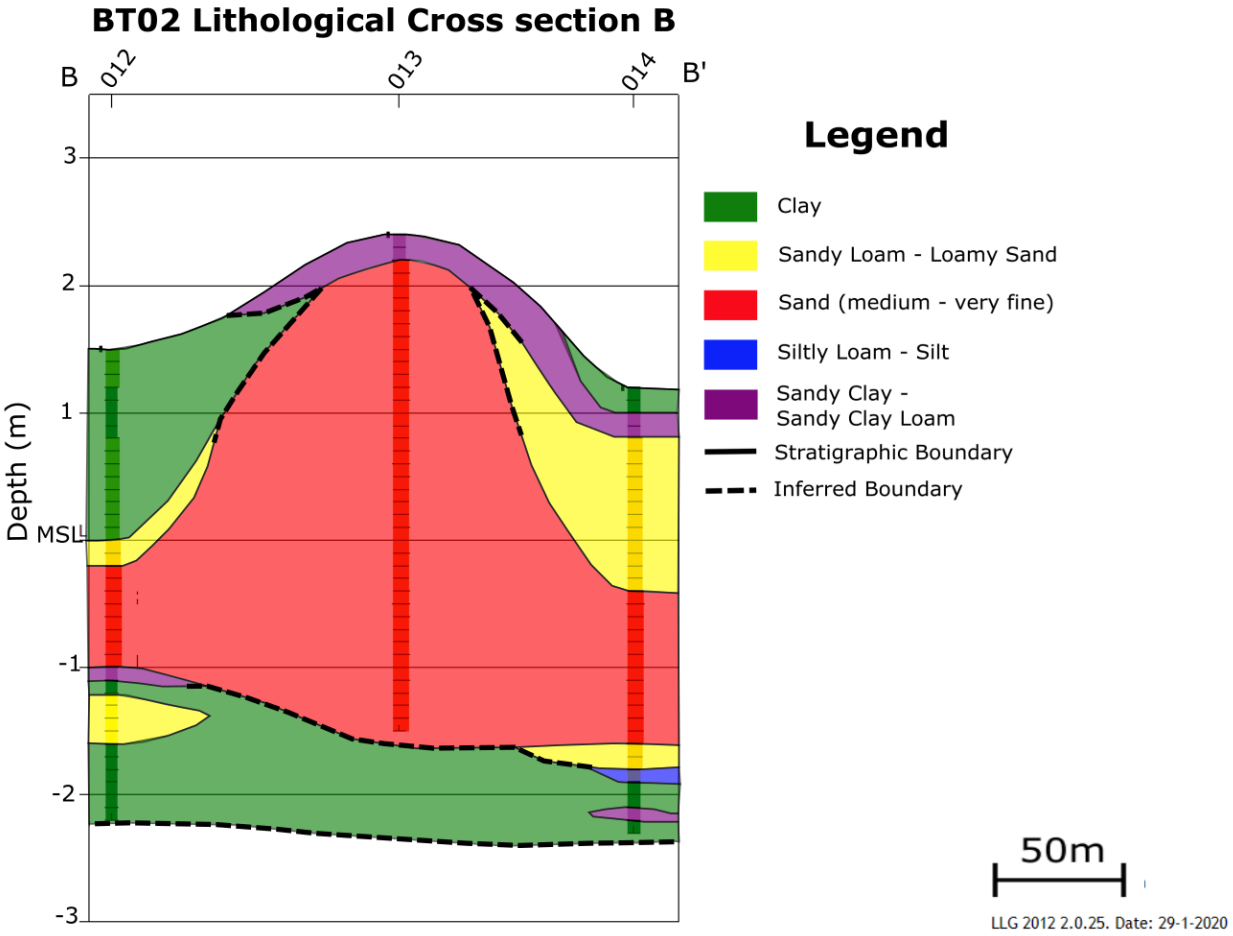

Figure 18). The clay deposits here (green) should be especially noted, as they are considered aquitards in the system. There is more consistency among cross sections 1 and 2 with the extent and thickness of the clay layers on the edges of the sandy ridge, than in cross section 3 (Figure 19), though they are still present. All three cross sections show the base of the system with an aquitard that is present between -1m and -2m below MSL. This is considered the system boundary for the unconfined aquifer and is assumed to be continuous. There is a single deep core in cross section 3 that depicts a potential confined aquifer, but as there is only one core, no definitive correlations can be made with this data, past the depth of the first aquitard.

4.1.3 Ridge Architecture of Tra Vinh field site TV02

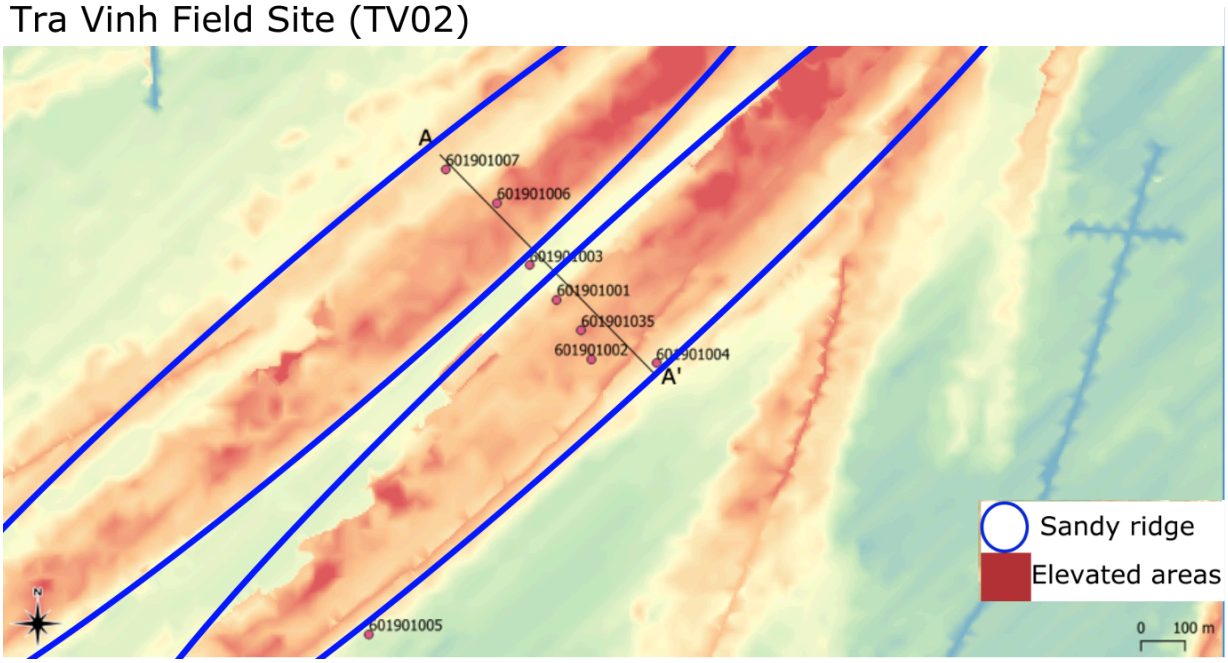

Figure 20 Elevation map depicting the sandy ridge structures of the TV02 site, with coring locations and cross section line.

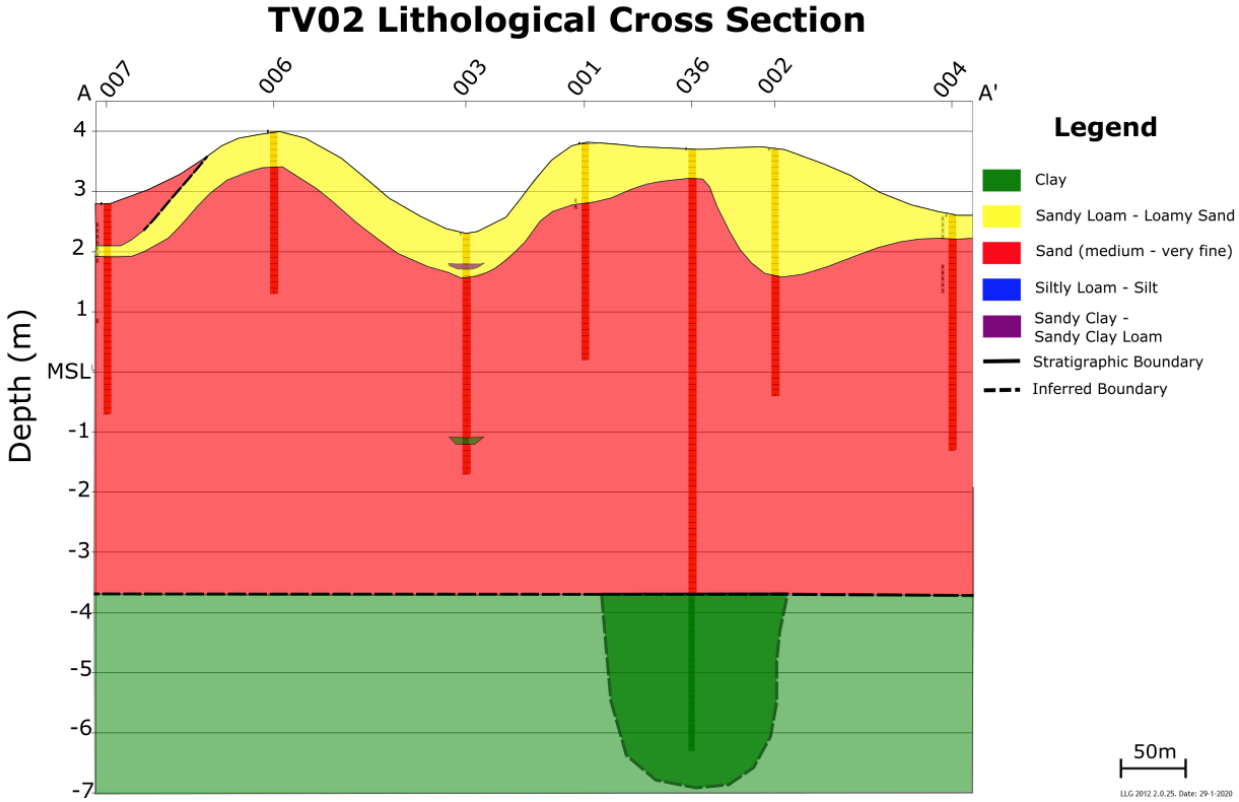

Figure 21 Cross section depicting subsurface interpretation of architecture, sediment types and boundaries, created using the LLG sofwere.

This site is characterized by a largely, deep and uniform sand layer of well sorted very fine sand (Figure 21). This was observed across two sandy ridge structures spanning approximately 670m. Very few clay deposits (maximum 20cm thick) were found during the shallow coring (maximum 4m deep). These small layers do not appear to be significant or continuous across the sandy ridges. The deep coring shows a thick clay layer, which is could be a continuous base of the sandy ridge, but this would only be an assumption based on what has been discovered about these systems. There is only one deep core that had the potential to reach the bottom system boundary, so no definitive correlations can be made across the system. In order to be able to calculate the storage capacity for the shallow aquifer, with more reliability, this boundary has to be assumed to be at the depth found by the depth core at 3.7m below MSL. Based on this boundary and varied surface elevation, the sand layer is approximately 7.4m – 6.2m thick.

4.1.1 Geological Observations

Core 031 (Appendix B) serves as a good example of sediments found in the field on a sandy ridge aquifer. Core 031 is obtained from deep drilling has the highest elevation (on top of the sandy ridge) of the cores logged in the field and is representative of sediments studied in the Ben Tre site (BT03). As only approximately 75% of samples are recovered during deep drilling, the exact depths of sedimentary observations have less confidence. Deep cores 031 and 032 also displayed good structural preservation in some areas when extracted.
In core 031, the uppermost ~3m consist of red brown fine - very fine, well sorted, sub angular, sand and show a fining upward sequence. Core 032 shows well preserved parallel laminations at approximately and an organic layer around 3m depth (Figure 27). There are also organics present in between 1.5 – 2.5m. A distinct color change to grey occurs at 3.6m, which is observed as the redoximorphic boundary, where the lowest groundwater level occurs. From 3.5m – 5m there is a layer of silty sands, very fine sands (poorly sorted), with clay (recorded as sandy clay loam). This layer also includes shells, shell fragments and mica flakes. This is followed by another layer of fine sand down to 8.5m, with an intermittent layer of sandy clay loam from 5.5 – 6.0m. More shells are present from 6.8 – 7m and shell fragments are present from 7.7 – 8.5m. There is an abrupt boundary separating the sand and clay at 8.5m. From 8.5m, to the bottom of the core, consist of clay. All core logs are available in the Appendix B.

4.2 Storage Capacity

An overview map of the sites is provided in Figure 5, and close up maps of the specific sandy ridges are displayed in section 4.1. Horizon line cross sections used to calculate storage capacity and storage capacity results are displayed in this section. This section is organized by presenting cross sections and storage capacity results for each site individually.

4.2.1 Capacity for BT03

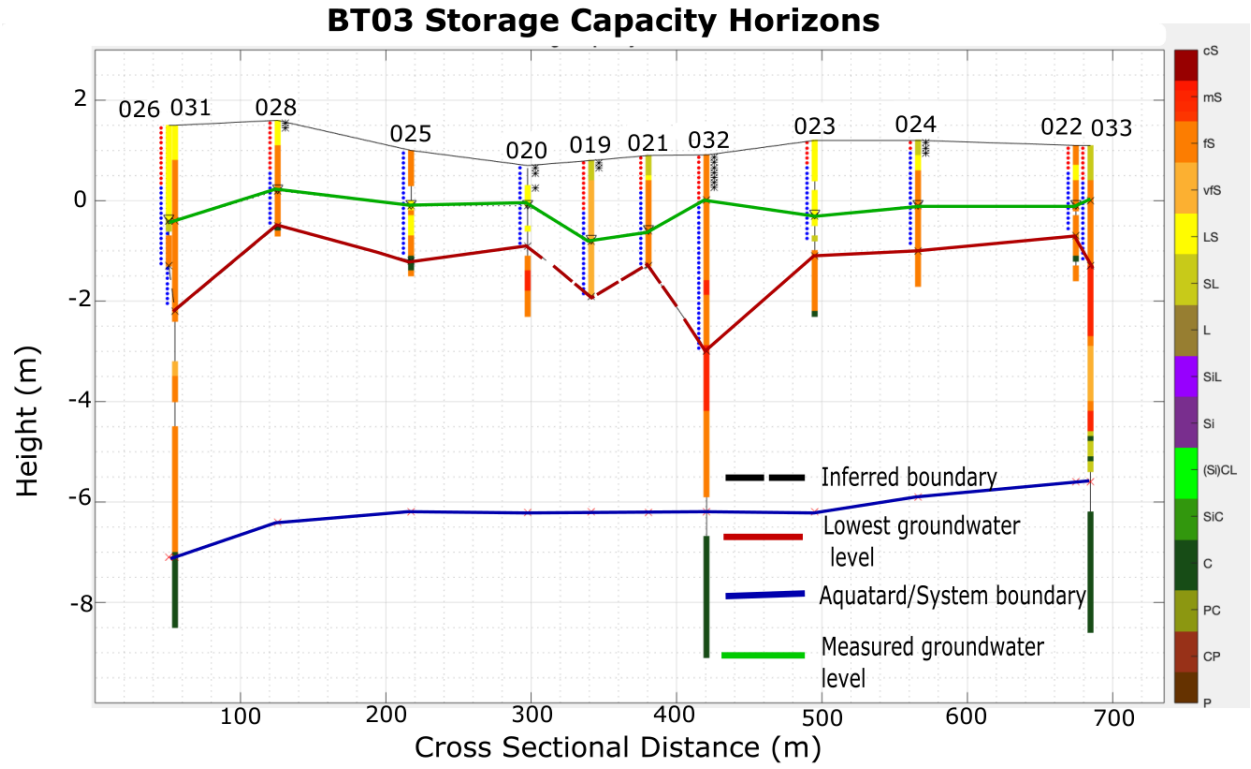

Figure 22 BT03 cross section depicting the surface level, groundwater level, lowest groundwater level and the base of the hydrogeological system. Created using a MATLAB program.

Table 4 BT03 Cross sectional area and storage calculations for maximum and minimum effective porosity values, and stretched perpendicular to the cross section.

BT03 Horizons	**Area**	**Min porosity volume per stretched m (m^3)**	**Max porosity Volume per stretched m (m^3)**	**Min Volume over 1000 meters (m^3)**	**Max Stretched Volume over 1000 meters (m^3)**
Surface-GW level	886	221	266	2.24E+05	2.68E+05

GW level – Low GW level	697	174	209	1.76E+05	2.11E+05
Total Aquifer	4635	1159	1391	1.17E+06	1.40E+06

The volume per stretched meter is extrapolated perpendicular across the length of the sandy ridge structure which is taken as approximately 1km. The BT03 site has the most cores and the most reliable hydrogeological data. This cross section is also having the highest density of cores and low groundwater table reading, so it has a much higher confidence and resolution, compared to the other sites. This cross section also includes three deep cores which all have a sharp contact with a clay aquitard at the base of the shallow aquifer. This contact is extrapolated across the system and used to calculate the total capacity of the aquifer from surface to base. It is worth mentioning core 027, which is the core furthest to the North, on the map (Figure 14). Core 027 is taken from a dugout field and consisted of at least 180m of a mix of sandy clay loam, and clay. This has the potential to be representative of a system boundary with more exploration, but as a single core of this type, high anthropogenic influence and poor recovery it is considered fairly unreliable. There is also a sharp redoximorphic feature representing the lowest groundwater level, in most all cores. This boundary is inferred in core 024, and core 025 in Figure 22, the remainder of the cores have this sharp contact. The lowest groundwater level horizon is the most accurate in this core. With this boundary it is possible to infer groundwater level fluctuations from the wet season to extreme dry seasons in this area. The groundwater table readings in this area were taken in early December, which is considered the dry season. The surface to groundwater level volume is representative of the potential capacity for infiltration in this site, depending on the availability and quality of fresh surface waters available for infiltration during this time.

4.2.2 Capacity for BT02

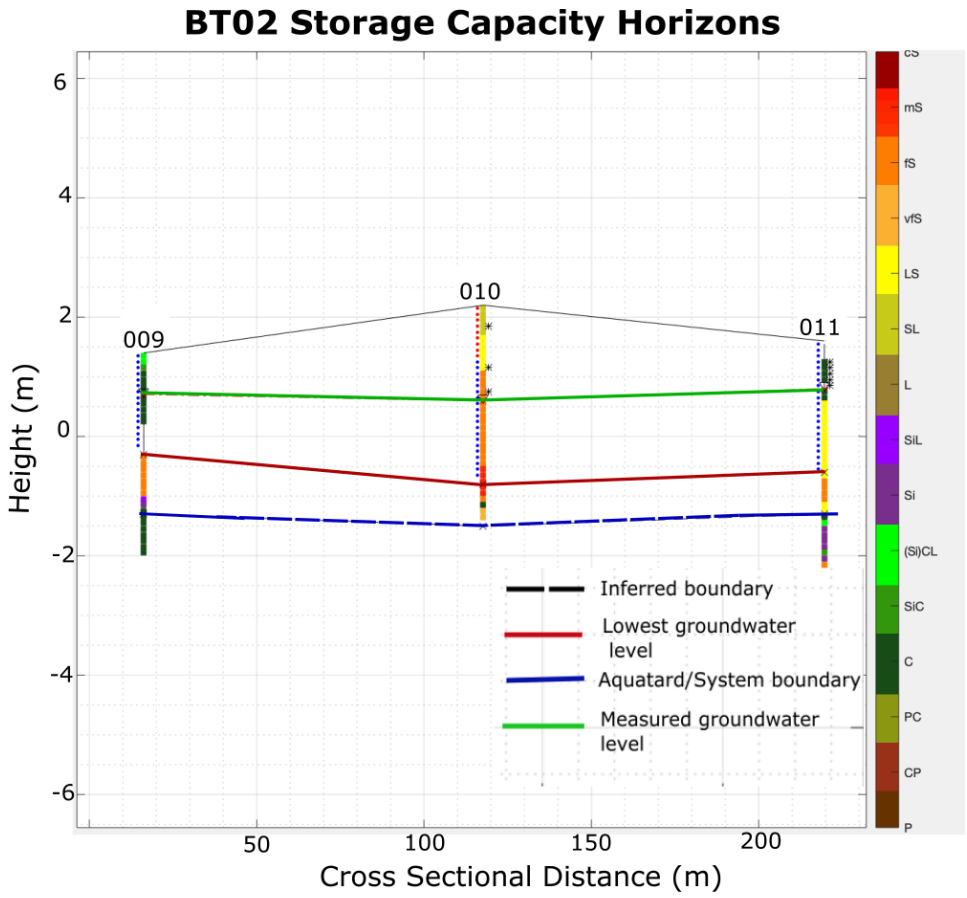

Figure 23 BT02 cross section depicting the surface level, groundwater level, lowest groundwater level and the base of the hydrogeological system. Created using a MATLAB program.

Table 5 BT02 Cross sectional area and storage calculations for maximum and minimum effective porosity values, and stretched perpendicular to the cross section.

BT02 Horizons	**Area**	**Min porosity volume per stretched m (m^3)**	**Max porosity Volume per stretched m (m^3)**	**Min Stretched Volume over 1500 meter (m^3)**	**Max Stretched Volume over 1500 meter (m^3)**
Surface-GW level	238	60	71	8.93E+04	1.07E+05
GW level – Low GW level	264	66	79	9.90E+04	1.19E+05
Total Aquifer	660	165	198	2.48E+05	2.97E+05

The volume per stretched meter is extrapolated perpendicular across the length of the sandy ridge structure which is taken as approximately 1.5km. This cross section presented with reliable lowest ground water level readings across all three cores. The aquitard / system boundary line extrapolated across the center core (core 10 in Figure 23) but is considered a fairly reliable

estimation as this boundary is found in nearby in other cores, as well as core 009 and 011. Looking at the deep core 034 in Figure 19, this aquitard may be quite thin, and may have connectivity to the lower confined aquifer. The resolution of the storage capacity horizons is reduced by the low number of cores in this cross section but considering the width (about 200m) of the feature itself the density of cores is reasonable. This site has the lowest storage capacity volume of all three sites by far, having only about 40% the surface to groundwater level storage capacity of the BT03 site.

4.2.3 Capacity for TV02

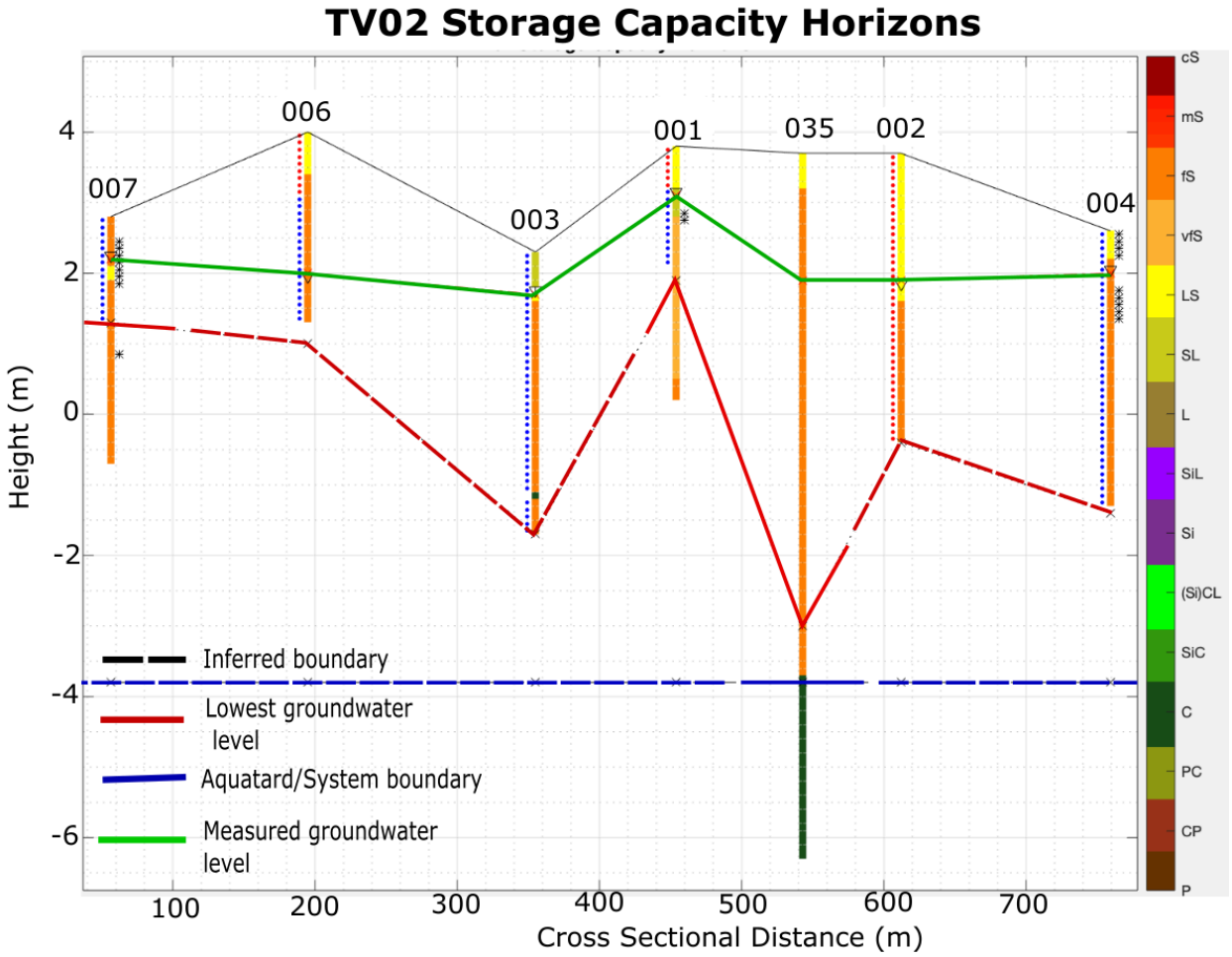

Figure 24 TV02 cross section depicting the surface level, groundwater level, lowest groundwater level and the base of the hydrogeological system. Created using a MATLAB program.

Table 6 TV02 Cross sectional area and storage calculations for maximum and minimum effective porosity values, and stretched perpendicular to the cross section.

TV02 Horizons	**Area**	**Min porosity volume per stretched m (m^3)**	**Max porosity Volume per stretched m (m^3)**	**Min Stretched Volume over 3000 meter (m^3)**	**Max Stretched Volume over 3000 meter (m^3)**
Surface-GW level	864	216	259	6.48E+05	7.78E+05
GW level – Low GW level	697	413	495	1.24E+06	1.49E+06
Total Aquifer	5000	1250	1500	3.75E+06	4.50E+06

The volume per stretched meter is extrapolated perpendicular across the length of the sandy ridge structure which is taken as approximately 3km. The storage capacity results from this site are considered the most unreliable. The lowest average groundwater reading, taken by the redoximorphic reduction zone boundary, was only found in 3 cores. This is not enough to extrapolate across the system with reasonable accuracy. The most reliable reading was the groundwater level, found in all coring locations. The most reliable results for the cross-sectional area is the surface to groundwater level. The ground water levels were taken in October, near the start of the dry season. This is also the zone that could be useable for infiltration of fresh water. The base of the system is assumed to be the aquitard in the deepest core (35 in Figure 24), and in order to estimate the cross-sectional area of sand in the system this is assumed to be continuous, which is not a reliable based on the single core, but this may be a valid assumption based on the similarities in the other deep cores. This site is largest sandy ridge studied and has largest storage capacity of the three sites.

4.3 Site suitability

The method outlined in 3.3.2 was used to evaluate each site in order to establish a way to give ratings to studied sites for a potential ASR system. The factors in Table 1 are used to assess the suitability of each site respectively. This scoring has been summarized in as well as the surface to ground water level storage capacity in Table 7.

Table 7 ASR suitability scoring and surface to GW level storage capacity for studied sites BT03, BT02, and TV02.

	Criteria	BT03	BT02	TV02
Factor A	Presence of elevated sandy geomorphological feature	1	1	1
Factor B	Unconfined aquifer	1	1	1
Factor C	Significantly comprised of homogenous sand	1	1	1
Factor D	Absence of extensional low flow layers within target aquifer	1	0	1
Factor E	Presence of horizontal and vertical aquifer boundaries	0	0	0
Factor F	Storage Capacity available during the end wet season with at least 0.85m of unsaturated zone).	1	0	1
Total Score		5	2	5
Suitability		Good	Low/possible	Good
Surface – GW lvl storage (max)		2.68E+05m^3	1.07E+05m^3	7.78E+05m^3

Table 7 represents the cumulative assessment of the subsurface outlined in this study. An aquifer that scores a 6 is considered ideal. Elevated sandy ridge aquifers (factors A and B) are shared by all sites. Being significantly comprised of sand (factor C) is a valuable component of an ASR system, for greater pore volume of the material and connectivity, which is why it is required for suitability. All three sites pass factor C. The significance of the sand is also based on the size of the sandy ridge, i.e. a small clay layer for a large ridge may be very large for a smaller sandy ridge. By observation of the subsurface cross sections, BT02 has the lowest fraction of sand. BT02 fails factor D (absence of low flow layers) due to the large clay layer that appears to separate the two larger sand layers. All sites fail for presence of horizontal and vertical boundaries (factor E), due to the absence and/ or the unknown existence of vertical boundaries,

but all are assumed to have horizontal boundaries. BT02 appears to have swale deposits, but, at their current extent, they do not appear to be vertically continuous. Factor F (0.85m of unsaturated zone during end wet season) is in place to ensure there is storage space available during the infiltration window, that will not cause root zone saturation or potential flooding of the lower areas. This factor is present for only TV02 and BT03 sites.

4.4 Aquifer storage and recovery potential map

The high saline risk areas are identified by utilizing the boolean maps created using the input maps in section 3.3.3. The three input boolean maps are multiplied together to create the resulting high saline risk map of elevated areas (Figure 25). The boolean salinity map of areas over 2.0 TDS g/L of salinity is used to identify the high saline risk elevated areas. The DEM map is set to identify areas above 1.5m, to ensure that the larger sandy ridges are accounted for. The land use map isolates areas that use irrigation in the dry season.

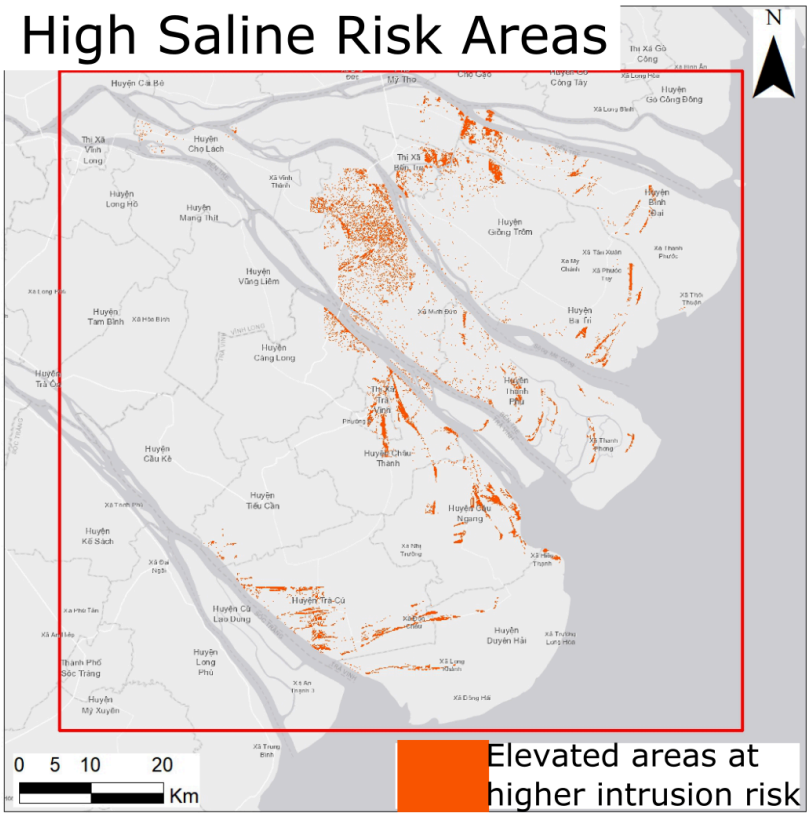

Figure 25 Output high saline risk boolean map from input maps of land use, salinity and elevation

The high saline risk area map does not correctly identify all sandy ridge structures in the target areas. It also does not separate sandy ridge structures from other elevated areas. To correct for this, the high saline risk areas map (Figure 25) is used in conjunction with a vector layer of (described in 3.3.3) to manually add in extended structures that intersect with the areas in Figure 25.

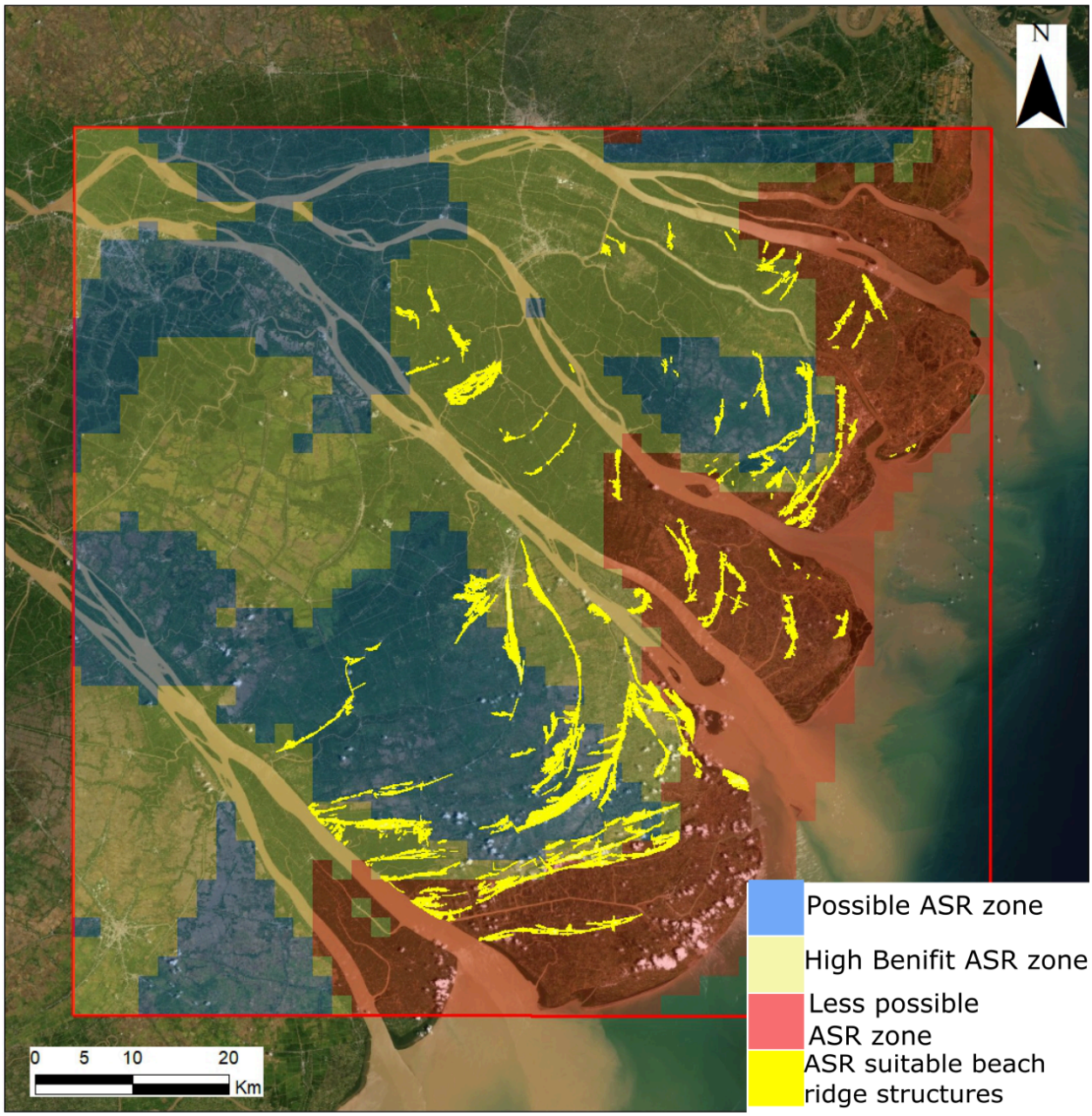

Figure 26 Sandy Ridge structure map with aquifer storage and recovery potential, based on surface water saltwater intrusion severity, elevated structures and land cover classes that irrigate during the dry season, in the Tra Vinh and Ben Tre provinces in the Vietnamese MKD.

The ASR potential map Figure 26 created shows elevated sandy ridge structures in areas deemed more suitable for increasing fresh water availability, categorized by the severity of saline intrusion in the surface water. The ASR potential map is overlain with the classified surface water salinity map. This shows which areas are having a high ASR benefit potential (light green), assumed to be too saline for ASR to be a practical solution (red), and areas that always have fresh water (blue) where ASR is assumed to be less necessary, but still possible depending on water availability. The final beach ridge with ASR benefit potential map produced shows the priority areas where additional exploration is recommended for ASR systems. These are areas sandy ridge structures (yellow) in the high benefit potential ASR zone (light green).

5 Discussion

5.1 Geological interpretation

It is possible to establish depositional settings and geologic context to the sandy ridges in the presented field sites by taking a detailed look at the cores and relating to literature, to understand the sediments of the sandy ridges, it's important to look at the depositional environments. To most accurately connect the cores gathered this study to another study, the work of Ta et al. will be considered, which concerns sediment facies classifications in a nearby cores in the Ben Tre province. These deposits are evident of a prograding delta and the formation of beach ridges. The observable layers within the deeper cores, namely 031 can be broken down into three facies: Delta front slope to pro delta, tidal flat deposits and the subaerial delta plain which includes beach ridges, interridge swales and floodplain deposits. The lowest being the delta front slope to pro delta deposits. These sediments are composed of dark grey silt and clay deposits, overlain by sand deposits with shells and shell fragments (Ta et al., 2002a). This is consistent with what is seen in the deeper cores, in BT03, where there is a thick layer of clay in the deeper areas. The boundary between the Delta front to pro delta sands and the tidal sands is more unclear in the shallow and deep cores obtained during this study, due to the recovery method, where the integrity of the sedimentary structures is easily lost. This layer is characterized by dark grey silty sands and fine sands, with a fining upward succession with a wide variation in sedimentary structures and with shell fragments and mica flakes (Ta et al., 2002a). In the cores taken from this study, evidence from this layer is the sands with mica flakes and shells that is distinctive from the upper and lower layers. The uppermost layer is the subaerial delta plain with interridge swales, floodplains and including the beach ridges, which is where the sites are based. This facies is characterized by discontinuous parallel lamination and lenticular bedding, and consists of fine yellowish brown sand, with some mica flakes and organic matter. (Ta et al., 2002a). This is also consistent with what was found during coring. There is one section of core (in core 031) with well-preserved parallel lamination structures from around 3m of depth, and a layer of organics at approximately 1.5m depth (photo included in the Appendix A, Figure 27). These three sedimentary facies compose the shallow unconfined aquifers that are of interest to this study and expansion of groundwater resource management with aquifer storage and recovery systems in the Mekong delta. In this study the strong color boundary in the cores (Figure 10), is taken as a redoximorphic feature based on a literature from (Vepraskas, 1992), but this is not mentioned in the works of Ta. et al or a rival explanation.

5.2 Site Suitability and Recommendations

In the presented lithological cross sections from the selected sites (section 4.1), the subsurface is visualized to evaluate how close they are to an ideal system. The cross sections represent an interpretation of what the subsurface could look like based on the coring logs. The most useful information obtained from these sections is the heterogeneity of the subsurface, the thickness of the sand aquifer and hydrogeological boundaries. It should be noted that the presence of vertical boundaries is largely absent section 4.1 and more exploration outward from the sandy ridges could prove the presence of swale deposits that could act as vertical boundaries.

The surface to groundwater level storage (section 4.2) capacity is assumed to be the volume available for fresh water infiltration at the time of the field campaign, at the start of the dry season. In theory this early dry season period represents the time when surface waters have low

salinity and there is storage volume available in the subsurface to infiltrate without the risk of flooding lower areas.

In section 4.3, it should be noted that both BT03 and TV02 are presented with the same score, but the confidence of the data from BT03 is much higher, as there are more cores, more deep cores and less inferred boundaries. TV02 is a promising site based on the evaluation, but the lower amount of data points requires more assumptions to be made about the geologic architecture of the site. For this reason, BT03 is the best candidate of the three. It is an unconfined, elevated aquifer comprised significantly of homogeneous sand, with minimal obstructive layers. It also has the most reliable horizontal hydrogeological boundary. This site has the most data associated with it from the field campaign, and therefore the results concerning BT03 are of a higher confidence than the other two sites. The storage volume available for infiltration between the groundwater level and the surface was estimated to be in between $6.5x10^5$ m^3 and $7.8x10^5 m^3$ for this site, and the water levels at the time of measurement were low enough to provide adequate space for infiltration. This seems to be the most geologically promising prospect for an ASR solution of the three sites, and additional information provided by the measurement infrastructure in place at the site will reveal its suitability with greater surety.

It is also important to consider factors for assessment that are not included in this study. Other students that participated in this initial field campaign of the FAME projected assessed these sites based on interviews concerning land and water use for agriculture, and hydrogeological and hydrological studies. To illustrate the importance of taking information from these sources as well the case of BT02 should be considered. While interesting geologically, it was found through interview that groundwater extraction at BT02 was predominantly being used for domestic use and some livestock, and not agriculture. The community also already has a water system provided by the government that supplements their supply in times of need. This kind of information also influences the suitability of an ASR system. Hydrogeological / hydrological measurement is also a vital component in assessment. There are rain gauges and piezometers installed on each of the three sites, that were installed during the field campaign, to gather information about water balance and groundwater fluctuations. These instruments will provide a better picture of water availability problems and the infiltration window. A probe was also used to make water quality measurements on the sites to find areas with quality problems and potential saline intrusion pathways. The quality of the water being infiltrated is important to consider. From interviews it was discovered that at the BT03 site, the residents also use the ground water as drinking water. Therefore, any water infiltrated needs to be of sufficient quality, not only for agriculture but also for human consumption. This serves as an example of how different areas of assessment for suitability can affect each other. It is clear that the assessment of the sites requires a multidisciplinary approach. In order to truly, define suitability the hydrological, hydrogeological, geological, agricultural and water use information have to be considered as a whole.

5.3 Improvement and further research

5.3.1 Field Methods

There are several challenges that future researchers should be aware of when considering additional field work. The suction coring only provided limited penetration due to the nature of the sediments. In order to reach the deeper parts of the aquifer, the suction coring was supplemented with deep cores, which were drilled by a professional team with a mechanical rig.

These deep cores are necessary to identifying the geological architecture of the shallow aquifer and hydrogeological boundaries. This kind of coring is preferable but is also very expensive and should therefore be used sparingly. The suction coring is useful for discovering sites that merit additional deeper exploration, but on larger sandy ridges it is evident that there is need for more deeper exploration to more accurately depict these structures. 4m of depth is not enough to adequately explore the boundaries of the larger sandy ridges. It may be possible to improve the build of the suction coring devices to go past this depth.

5.3.2 Storage Capacity

The storage capacity calculations are based on cross sections from each site. The resolution of the storage capacity could be greatly improved by utilizing more cross sections for each site. This way the volume measurements of the sedimentary layers could be mapped and analyzed in 3D using a software such as iMOD (Vermeulen et al. 2020). The MATLAB software is a very useful tool for analyzing cross sections and provides a way to customize and add horizon lines that can be easily used for analysis. Instead of integrating the area between curves, as the MATLAB program does, it's possible that program could be improved by using using a coordinate geometry method called Gauss' area formula (Persson et al., 2006).

$$\mathrm{A} = \sum_{i=1}^{n} (X_{i+1} Y_i - X_i Y_{i+1})$$

This way, layers which are not continuous across the system could be accounted for when determining storage capacity. The estimation of the storage capacity in this report is provided as a range to account for uncertainties in effective porosity. The grain size observed in the field, is not an accurate portrayal of the sediment size distribution in the subsurface. The field measurements account for the average grain size, as the fewer smaller and larger particles are not accounted for by using a sand ruler. To improve this, grain size distribution can be obtained through sieve analysis or laser diffraction of samples. The grain size of the material has no influence on effective porosity, but the grain size distribution does have an effect of effective porosity. Smaller grains can fill voids between larger grains, which changes porosity. Sorting, packing shape and roundness also have an effect on the volume of pore space between grains (Gibb et al., 1984). A more useful parameter to obtain may be specific yield of the material in question. This is where specific yield is the difference between the total porosity and the residual soil water content left in the material once it is drained (specific retention). Specific yield is a useable substitute for effective porosity in shallow soils (Gibb et al., 1984).
Important hydrogeologic factors such as storativity, transmissivity and hydraulic conductivity, could be estimated with pumping tests. The deeper drillings were all completed with well casings and screens with piezometers. These wells could be used to obtain more hydrogeologic data from pumping tests, as well as head fluctuation data, to create a hydrogeological assessment of the aquifer, that gives a more comprehensive view about how these systems function. The infrastructure for additional assessment, and long-term evaluation was set up during the field campaign and is intended to be used by future researchers.

5.3.3 ASR potential mapping

The ASR potential map is provided in this thesis as a point for further exploration of sandy ridge structures in the Ben Tre and Tra Vinh provinces that could benefit from an ASR system. This map can be further refined by including more factors, such as land availability, water usage, and

economic potential, which will narrow down the suitability area. The land use map does not seem to always accurately account for built up areas, and it can be difficult to distinguish from built up areas and sandy ridge areas. Some built up areas appear to be built on top of the sandy ridges, with a road running on the crest of the sandy ridge. BT02 serves as an example of this. These types of areas may not be suitable for ASR if there are too may man-made obstructions to install the system. In the current map, more built up areas are manually eliminated by comparing elevated shapes to satellite images. The map may further be improved by implementing a groundwater salinity map for the first 10 m or so. This way it may be evident which sandy ridge aquifers are being contaminated with salt water. If there were data available detailing surface sediment types, there is potential for identification of other sandy shallow aquifers, and interridge swale deposits. The suitability could be refined and potentially expanded with this information.

It is assumed that ridges in areas with high surface saltwater intrusion are less feasible for ASR solutions (Figure 26). This is because saltwater intrusion is assumed to come earlier in these areas, and with a higher salt concentration. Therefore, the infiltration window will be smaller, transitioning form the wet to dry season (late November – December), and the quality of the water available for infiltration will be lower. The possible ASR zones are, fresh water zones. These are considered less likely to benefit from ASR as the salinity levels are low. This does not necessarily mean that they cannot benefit from ASR solutions. ASR can supply improved water quantities as well as quality. The fresh water areas may also see quality/quantity declines with climate change. The map does not account for, declining head levels, droughts, or other aquifer problems like contamination, high metal concentrations, excessive drawdown, etc. In the map presented ASR is still considered possible on a case by case basis.
The salinity map from 2016 is used to represent problematic conditions in the Mekong Delta. An aquifer storage and recovery solution has the potential to combat these kind of conditions and increase water security, in times of need. The potential map may yield the identification of communities that can benefit the most, as groundwater insecurity increases in the MKD.

6 Conclusions

The expansion and economic growth of the delta has put a strain on groundwater supply that the people depend on for food, and prosperity. The VMD will continue to be impacted by water scarcity with more groundwater extraction, subsidence, climate change, sea level rise, and saltwater intrusion of groundwater and surface water systems. These problems will persist with increasing severity, without bridging the gap between increased fresh water demand and supply. The aim of this research is to provide a basis of understanding with geological/hydrogeological field research and suitability mapping, that can be used to evaluate the feasibility of aquifer storage and recovery systems in the provinces of Tra Vinh and Ben Tre in the Vietnamese Mekong Delta. This was done by answering the following research question through three sub questions:

What is the hydrogeological potential of the shallow sandy ridge aquifers in the Vietnamese Mekong Delta for local aquifer storage and recovery solutions?

1. What is the geological architecture of the sandy ridge aquifers found in the Tra Vinh and Ben Tre provinces?

The architecture was studied by utilizing deep and shallow coring data to create and interpret cross sections across three sites. The sandy ridges are unconfined, shallow aquifers, identified by their elongated elevated structure, composed predominantly of fine sand, with a clay layer, acting as an aquitard, at the base of the system. This aquitard has the highest confidence in the BT03 site. Thickness of the sand layers and intermittent layers are variable from site to site. Sand thickness and depth to confining layer are used to calculate storage.

2. What is the capacity for water storage in the shallow sandy ridge ground water systems?

The storage capacity of each was assessed by utilizing hydrogeological horizons and calculating areas between them using a range of effective porosities. These values were then extrapolated perpendicular to the length of the cross section to give a min and max storage capacity for each site. The surface level to groundwater level is considered the available room for infiltration of fresh water.

3. What areas are most suitable for ASR solutions in the Tra Vinh and Ben Tre provinces?

A suitability map was created to find sandy ridges in areas deemed most suitable for ASR solutions, using information on elevation, land use and surface water salinity intrusions. The map considers areas, with elevated dune structures, that irrigate in the dry season, and have marginal to saline salt water intrusions in surface waters, to be the areas that can benefit most from an ASR solution.

A rating system was established to compare studied aquifers to the ideal site for an ASR system. The three sites in Tra Vinh (TV02) and Ben Tre (BT02 and BT03) were evaluated for ASR suitability utilizing this rating system. The geologic architecture of the BT03 site proved the most feasible for ASR, because it passes the following factors; presence of elevated sandy geomorphological feature, unconfined aquifer, significantly comprised of homogeneous sand,

absence of extensional low flow layers, and storage capacity available during the end of the wet season. This site also has the most reliable horizontal hydrogeological boundary, evident by the presence of a clay layer that exists across three deep corings. The suitability map created provides a way to find new sites that have the potential to benefit from ASR solutions. The success of an ASR solution has the potential to protect residence from economic damage and, in extreme cases, food insecurity. Exploring this system of water management in Vietnamese Mekong Delta, could aid in the security of water resources for many farmers in increasingly uncertain times.

7 References

Boretti, A. 2020. Implications on food production of the changing water cycle in the Vietnamese Mekong Delta. Glob. Ecol. Conserv. 22: e00989. doi: 10.1016/j.gecco.2020.e00989.

CGIAR, R.C. in S.A. 2016. The drought and salinity intrusion in the Mekong River Delta of Vietnam Assessment Report CGIAR Research Centers in Southeast Asia. (April): 55. https://cgspace.cgiar.org/rest/bitstreams/78534/retrieve.

Delsman, J.R., J.M. De Paz, M. De Klerk, L. Stuyt, P.G.B. de Louw, et al. 2015. Application of the FWOO method in the Vega Baja Segura catchment Application of the FWOO method in the Vega Baja Segura catchment.

Eslami, S., P. Hoekstra, N. Nguyen Trung, S. Ahmed Kantoush, D. Van Binh, et al. 2019. Tidal amplification and salt intrusion in the Mekong Delta driven by anthropogenic sediment starvation. Sci. Rep. 9(1): 1–10. doi: 10.1038/s41598-019-55018-9.

Fetter, C.W. 2018. Applied Hydrogeology: Fourth Edition. 4th ed. Waveland Press.

Foufoula-Georgiou, E. 2013. A vision for a coordinated international effort on delta sustainability. IAHS-AISH Proc. Reports 358(July): 3–11.

Gibb, J.P., M.J. Barcelona, J.D. Ritchey, and M.H. LeFaivre. 1984. Effective porosity of geologic materials: First annual report.

Hamer, T., C. Dieperink, V.P.D. Tri, H.S. Otter, and P. Hoekstra. 2020. The rationality of groundwater governance in the Vietnamese Mekong Delta's coastal zone. Int. J. Water Resour. Dev. 36(1): 127–148. doi: 10.1080/07900627.2019.1618247.

Jiménez Cisneros, B.E., T. Oki, N.W. Arnell, G. Benito, J.G. Cogley, et al. 2014. 2014: Freshwater resources. Climate Change 2014: Impacts, Adaptation, and Vulnerability. Part A: Global and Sectoral Aspects. Contribution of Working Group II to the Fifth Assessment Report of the Intergovernmental Panel on Climate Change

Käkönen, M. 2008. Mekong Delta at the Crossroads: More Control or Adaptation? Ambio 37: 205–212. doi: 10.1579/0044-7447(2008)37[205:MDATCM]2.0.CO;2.

Kuenzer, C., H. Guo, J. Huth, P. Leinenkugel, X. Li, et al. 2013. Flood mapping and flood dynamics of the mekong delta: ENVISAT-ASAR-WSM based time series analyses. Remote Sens. 5(2): 687–715. doi: 10.3390/rs5020687.

Mayer, X., J. Ruprecht, and M. Bari. 2005. Stream salinity status and trends in south-west Western Australia. Changes: 188.

Minderhoud, P.S.J. 2019. The sinking mega-delta; Present and future subsidence of the Vietnamese Mekong delta.

Minderhoud, P.S.J., L. Coumou, L.E. Erban, H. Middelkoop, E. Stouthamer, et al. 2018. The relation between land use and subsidence in the Vietnamese Mekong delta. Sci. Total Environ. 634: 715–726. doi: 10.1016/j.scitotenv.2018.03.372.

Minderhoud, P.S.J., L. Coumou, G. Erkens, H. Middelkoop, and E. Stouthamer. 2019a. Mekong delta much lower than previously assumed in sea-level rise impact assessments. Nat. Commun. 10(1): 1–13. doi: 10.1038/s41467-019-11602-1.

Minderhoud, P.S.J., G. Erkens, V.H. Pham, V.T. Bui, L. Erban, et al. 2017. Impacts of 25 years of groundwater extraction on subsidence in the Mekong delta, Vietnam. Environ. Res. Lett. 12(6). doi: 10.1088/1748-9326/aa7146.

Minderhoud, P.S.J., G. Erkens, V.H. Pham, B.T. Vuong, and E. Stouthamer. 2015. Assessing the

potential of the multi-Aquifer subsurface of the Mekong Delta (Vietnam) for land subsidence due to groundwater extraction. Proc. Int. Assoc. Hydrol. Sci. 372: 73–76. doi: 10.5194/piahs-372-73-2015.
Minderhoud, P.S.J. (Philip S.J., H. (Hans) Middelkoop, and Universiteit Utrecht. Faculteit Geowetenschappen. 2019b. The sinking mega-delta : present en future subsidence of the Vietnamese Mekong delta = De zinkende mega-delta : huidige en toekomstige bodemdaling in de Vietnamese Mekong delta.
Nguyen, N.A. 2017. Lessons learned and response solutions. Vietnam J. Sci. Technol. 1(1): 2015–2018.
Nicholls, R., P.P. Wong, V. Burkett, J.O. Codignotto, J. Hay, et al. 2007. Coastal systems and low-lying areas. Fac. Sci. - Pap.
Oude Essink, G.H.P., E.S. Van Baaren, K.G. Zuurbier, J. Velstra, J. Veraart, et al. 2018. GO-FRESH: Valorisatie kansrijke oplossingen voor een robuuste zoetwatervoorziening. : 84.
Pauw, P.S., E.S. van Baaren, M. Visser, P.G.B. de Louw, and G.H.P. Oude Essink. 2015. Increasing a freshwater lens below a creek ridge using a controlled artificial recharge and drainage system: a case study in the Netherlands. Hydrogeol. J. 23(7): 1415–1430. doi: 10.1007/s10040-015-1264-z.
Persson, A.H., L. Bondesson, and N. Börlin. 2006. Estimation of Polygons and Areas. Scand. J. Stat. 33(3): 541–559. http://www.jstor.org/stable/4616941.
Pham, H. Van, F.C. Van Geer, V. Bui, and W. Dubelaar. 2019. Journal of Hydrology : Regional Studies Paleo-hydrogeological reconstruction of the fresh-saline groundwater distribution in the Vietnamese Mekong Delta since the late Pleistocene. J. Hydrol. Reg. Stud. 23(February): 100594. doi: 10.1016/j.ejrh.2019.100594.
Rahman, M.M., G. Penny, M.S. Mondal, M.H. Zaman, A. Kryston, et al. 2019. Salinization in large river deltas: Drivers, impacts and socio-hydrological feedbacks. Water Secur. 6(February): 100024. doi: 10.1016/j.wasec.2019.100024.
Rambags, F., K.J. Raat, K.G. Zuurbier, G.A. van den Berg, and N. Hartog. 2013. Aquifer Storage and Recovery (ASR). Design and operational experiences for water storage through wells. (February 2016). http://www.prepared-fp7.eu/viewer/file.aspx?FileInfoID=436.
Renaud, F.G., T.T.H. Le, C. Lindener, V.T. Guong, and Z. Sebesvari. 2015. Resilience and shifts in agro-ecosystems facing increasing sea-level rise and salinity intrusion in Ben Tre Province, Mekong Delta. Clim. Change 133(1): 69–84. doi: 10.1007/s10584-014-1113-4.
Sebastian, L., B.O. Sander, E. Simelton, S. Zheng, C. Hoanh, et al. 2016. The drought and salinity intrusion in the Mekong River Delta of Vietnam - Assessment report.
Sommeijer, M.J. 2012. Identifying suitable measures to enlarge fresh groundwater reserves on a regional scale; A feasibility study in Walcheren, the Netherlands. (February).
Ta, T.K.O., V.L. Nguyen, M. Tateahi, I. Kobayashi, and Y. Saito. 2011. Holocene Delta Evolution and Depositional Models of the Mekong River Delta, Southern Vietnam. River Deltas-Concepts, Model. Examples (41476049): 453–466. doi: 10.2110/pec.05.83.0453.
Ta, T.K.O., V.L. Nguyen, M. Tateishi, I. Kobayashi, Y. Saito, et al. 2002a. Sediment facies and Late Holocene progradation of the Mekong River Delta in Bentre Province, southern Vietnam: An example of evolution from a tide-dominated to a tide- and wave-dominated delta. Sediment. Geol. 152(3–4): 313–325. doi: 10.1016/S0037-0738(02)00098-2.
Ta, T.K.O., V.L. Nguyen, M. Tateishi, I. Kobayashi, S. Tanabe, et al. 2002b. Holocene delta

evolution and sediment discharge of the Mekong River, southern Vietnam. Quat. Sci. Rev. 21(16–17): 1807–1819. doi: 10.1016/S0277-3791(02)00007-0.

Tamura, T., Y. Saito, M.D. Bateman, V.L. Nguyen, T.K.O. Ta, et al. 2012. Luminescence dating of beach ridges for characterizing multi-decadal to centennial deltaic shoreline changes during Late Holocene, Mekong River delta. Mar. Geol. 326–328: 140–153. doi: 10.1016/j.margeo.2012.08.004.

Vepraskas, M.J. 1992. Redoximorphic features for identifying aquic conditions. North Carolina Agric. Res. Serv. Tech. Bull. 0(301): I–III, 1–33.

Wagner, F., F.G. Renaud, and V. Bui Tran. 2012. The Mekong Delta System (F.G. Renaud and C. Kuenzer, editors). Springer Netherlands, Dordrecht.

Wallinga, J., and J. van der Staay. 1999. Sampling in waterlogged sands with a simple hand-operated corer. Anc. TL 17(2): 59–61.

Wong, P.P., I.J. Losada, J.-P. Gattuso, J. Hinkel, A. Khattabi, K.L. McInnes, Y. Saito, and A. Sallenger, 2014. 2014. Coastal systems and low-lying areas. In: Field, C.B., Barros, V.R., Dokken, D.J., Mach, K.J., and Mastrandrea, M.D., editors, Climate Change 2014 Impacts, Adaptation and Vulnerability: Part A: Global and Sectoral Aspects. Cambridge University Press, Cambridge. p. 361–410

Zuurbier, K.G., J.W. Kooiman, M.M.A. Groen, B. Maas, and P.J. Stuyfzand. 2015. Enabling successful aquifer storage and recovery of freshwater using horizontal directional drilled wells in coastal aquifers. J. Hydrol. Eng. 20(3). doi: 10.1061/(ASCE)HE.1943-5584.0000990.

8 Appendix

8.1 Appendix A

Van der Staay Construction and Use

The Staays were constructed on site utilizing PVC tubing, clamps with handles, wooden plugs, washers, screws, and leather discs. The Staays consist of an inner tube that acts as a plunger to create suction and an outer tube with a handle that acts as a casing for the sediment. The Staay is prepared by wetting the leather ends in water and then inserting the inner tube inside the outer, leaving a few cm gap between the two tubes at the coring end. The Staay is placed into the borehole and its depth is recorded before extractions. The operation procedure of this follows the same steps described by (Wallinga and van der Staay, 1999). A wedge is placed in-between the two tubes to prevent slipping. Then the outer tube is pushed down using the handles while the inner tube pulled slightly upwards, while keeping its position as much as possible. When at the desired depth, the wedge is placed back between the tubes and the tubes are extracted and placed horizontal as quickly as possible to prevent sediment loss. The core can then be pushed out by holding the position of the inner tube and pulling the outer tube over it.

Sedimentary Structures found in Deep core 032

Figure 27 Planar lamination sedimentary structure found in core 032.

Organic layer found in deep core 032

Figure 28 Well preserved layer of organics observed in deep core 032

Close up of sediments from BT03

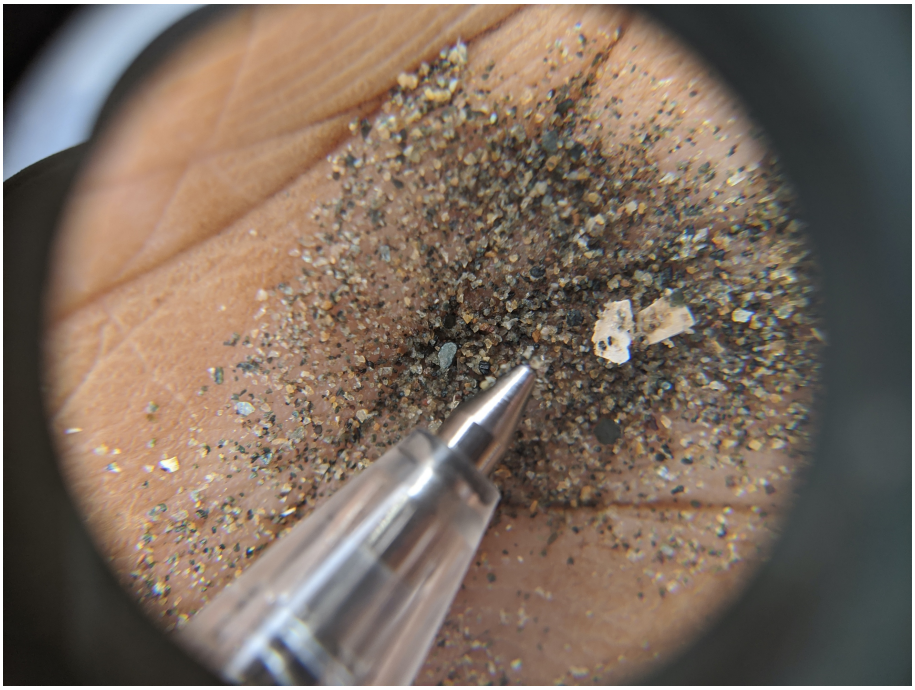

Figure 29 Typical sediment found past 3m in the BT03 site, containing small mica flakes, and shell fragments.

Example of a deep core (032)

Figure 30 Example of a deep coring from the Ben Tre field site (BT03)

8.2 Appendix B

Core Logs

Referred to by last three numbers in the borehole header in the top right of the log.

Borehole: 601901031 Names: Josh Year: 6019 Group: 01 Date: 12-12-2019

Coordinates		Elevation	Depth
XCO	YCO	Z [m]	[cm]
663125	1120215	1,5	1000

MAP LEGEND CODE	Geomorphogenetical map:
Geological map:	Groundwaterstep:
Vegetation-map:	Soil map:

1st deep coring in BT03, they retain 75% of the samples, in the farmers yards w/ the fruit trees. B1

Depth	Texture	Org	Plr	Color	Redox	Gravel	M50	Ca	Fe	GW	M	LKL	Strat	Remarks
10	LS			lbr	o		75-105	0	1					
20	LS			lbr	o		75-105	0	1					
30	LS			lbr	o		75-105	0	1					
40	LS			lbr	o		75-105	0	1					
50	LS			lbr	o		75-105	0	1					
60	LS			lbr	o		75-105	0	1					
70	LS			lbr	o		75-105	0	1					
80	fS			rdbr	o		105-150	0	1					
90	fS			rdbr	o		105-150	0	1					
100	fS			rdbr	o		150-210	0	1					
110	fS			rdbr	o		150-210	0	1					vws, sa-a
120	fS			rdbr	o		150-210	0	1					
130	fS			rdbr	o		150-210	0	1					(photo)
140	fS			rdbr	o		150-210	0	1					
150	fS			rdbr	or		150-210	0	1	GHG				
160	fS			rdbr	or		150-210	0	1					org
170	fS			rdbr	or		150-210	0	2					
180	fS			rdbr	or		150-210	0	2					
190	fS			rdbr	or		150-210	0	2					
200	fS			rdbr	or		150-210	0	2					
210	fS			rdbr	or		150-210	0	2					org
220	fS			rdbr	or		150-210	0	1					org
230	fS			rdbr	or		150-210	0	1					
240	fS			rdbr	or		150-210	0	1					
250	fS			rdbr	or		150-210	0	1					
260	fS			rdbr	or		150-210	0	2					
270	fS			rdbr	or		150-210	0	2		8			
280	fS			rdbr	or		150-210	0	2					
290	fS			rdbr	or		150-210	0	2					
300	fS			rdbr	or		150-210	0	2					
310	fS			rdbr	or		150-210	0	2					
320	fS			rdbr	or		150-210	0	2					
330	fS			rdbr	or		150-210	0	2					
340	fS			rdbr	or		150-210	0	2					
350	fS			rdbr	or		105-150	0	2					
360	fS			rdbr	or		105-150	0	2					shells
370	fS			gr	r		105-150	1	0	GLG				ps, sa-a, shells
380	fS			gr	r		105-150	1	0					shells
390	fS			gr	r		105-150	1	0					(photo), shells
400	SCL			gr	r		75-105	1	0					shells
410	SCL			dgr	r		75-105	0	0		7			shells
420	SCL			gr	r		75-105	0	0					shells
430	SCL			gr	r		75-105	0	0					clay clasts, shells
440	SCL			gr	r		75-105	0	0					clay clasts, shells
450	SCL			gr	r		75-105	0	0					clay clasts, shells
460	SCL			gr	r		75-105	0	0					clay clasts, shells
470	SCL			gr	r		75-105	0	0					shells
480	vfS			gr	r		75-105	0	0					shells
490	vfS			gr	r		75-105	0	0					shells
500	vfS			gr	r		75-105	0	0					shells
510	fS			gr	r		150-210	0	0					
520	fS			gr	r		150-210	0	0					
530	fS			gr	r		150-210	0	0					
540	fS			gr	r		150-210	0	0					
550	fS			gr	r		150-210	0	0					

Borehole: 601901031

Depth	Texture	Org	Plr	Color	Redox	Gravel	M50	Ca	Fe	GW	M	LKL	Strat	Remarks
560	SCL			gr	r			0	0		9			
570	SCL			gr	r			0	0					
580	SCL			gr	r			0	0					
590	SCL			gr	r			0	0					
600	SCL			gr	r			0	0					
610	fS			gr	r		150-210	0	0					
620	fS			gr	r		150-210	0	0					
630	fS			gr	r		150-210	0	0					
640	fS			gr	r		150-210	0	0					
650	fS			gr	r		150-210	0	0					
660	fS			gr	r		150-210	0	0					
670	fS			gr	r		150-210	0	0					
680	fS			gr	r		150-210	0	0					shells
690	fS			gr	r		150-210	0	0					shells
700	fS			gr	r		150-210	0	0					shells
710	fS			gr	r		150-210	0	0					
720	fS			gr	r		150-210	0	0					
730	fS			gr	r		150-210	0	0					
740	fS			gr	r		150-210	0	0					
750	fS			gr	r		150-210	0	0					
760	fS			gr	r		150-210	0	0					
770	fS			gr	r		150-210	0	0					
780	fS			gr	r		150-210	0	0					shell frag
790	fS			gr	r		150-210	0	0					shell frag
800	fS			gr	r		150-210	0	0		10			shell frag
810	fS			gr	r		150-210	0	0					shell frag
820	fS			gr	r		150-210	0	0					shell frag
830	fS			gr	r		150-210	0	0					shell frag
840	fS			gr	r		150-210	0	0					
850	fS			gr	r		150-210	0	0					
860	C			gr	r			0	0					
870	C			gr	r			0	0					
880	C			gr	r			0	0					
890	C			gr	r			0	0					
900	C			gr	r			0	0					
910	C			gr	r			0	0					
920	C			gr	r			0	0					
930	C			gr	r			0	0					
940	C			gr	r			0	0					
950	C			gr	r			0	0					
960	C			gr	r			0	0					
970	C			gr	r			0	0					
980	C			gr	r			0	0					
990	C			gr	r			0	0					
1000	C			gr	r			0	0					

End of borehole: 601901031

Borehole: 601901032 Names: Josh Year: 6019 Group: 01 Date: 13-12-2019

Coordinates		Elevation	Depth
XCO	YCO	Z [m]	[cm]
663079	1119956	0,91	1000

MAP LEGEND CODE	Geomorphogenetical map:
Geological map:	Groundwaterstep:
Vegetation-map:	Soil map:

BT03 Core A1?, by farmer with fruit tress beside the main farm, on top of the dune same as core 21

Depth	Texture	Org	Plr	Color	Redox	Gravel	M50	Ca	Fe	GW	M	LKL	Strat	Remarks
10	fS		plr	lbr	o		150-210	0	1					
20	fS		plr	lbr	o		150-210	0	1					
30	fS		plr	lbr	o		150-210	0	1					
40	fS		plr	lbr	o		150-210	0	1					
50	fS		plr	lbr	o		150-210	0	1					
60	fS		plr	lbr	o		150-210	0	1					
70	fS		plr	lbr	o		150-210	0	1					
80	fS			br	o		150-210	0	1					
90	fS			br	o		150-210	0	1					
100	fS			br	o		150-210	0	1					
110	fS			br	or		150-210	0	1					
120	fS			br	or		150-210	0	1					
130	fS			br	or		150-210	0	2					
140	fS			br	or		150-210	0	2					
150	fS			br	or		150-210	0	2					
160	fS			br	or		150-210	0	2					
170	fS			br	or		150-210	0	2					
180	fS			br	or		150-210	0	2					
190	fS			br	or		150-210	0	2					
200	fS			br	or		150-210	0	2					
210	fS			br	or		150-210	0	1					
220	fS			br	or		150-210	0	1					
230	fS			br	or		150-210	0	1					
240	fS			br	or		150-210	0	1					
250	fS			br	or		150-210	0	1					
260	mS			rdbr	or		210-300	0	2					
270	mS			rdbr	or		210-300	0	2					
280	mS			rdbr	or		210-300	0	2		11			iron bands
290	fS			rdbr	or		150-210	0	2					org strip (pic)
300	fS			br	or		150-210	0	1					
310	fS			br	or		150-210	0	1					
320	fS			br	or		150-210	0	1					
330	fS			br	or		150-210	0	1					
340	fS			br	or		150-210	0	1					
350	fS			br	or		150-210	0	1					
360	fS			br	or		150-210	0	1					
370	fS			br	or		150-210	0	1					
380	fS			br	or		150-210	0	1					
390	mS			grbr	or		210-300	0	0	GLG				
400	mS			gr	r		210-300	0	0					
410	mS			gr	r		210-300	0	0					
420	mS			gr	r		210-300	0	0					
430	mS			gr	r		210-300	0	0					
440	mS			gr	r		210-300	0	0					
450	mS			gr	r		210-300	0	0					
460	mS			gr	r		210-300	0	0		12			
470	mS			gr	r		210-300	0	0					
480	mS			gr	r		210-300	0	0					
490	mS			gr	r		210-300	0	0					
500	mS			gr	r		210-300	0	0					
510	mS			gr	r		210-300	0	0					
520	fS			gr	r		150-210	0	0					
530	fS			gr	r		150-210	0	0					
540	fS			gr	r		150-210	0	0					
550	fS			gr	r		150-210	0	0					

Borehole: 601901032

Depth	Texture	Org	Plr	Color	Redox	Gravel	M50	Ca	Fe	GW	M	LKL	Strat	Remarks
560	fS			gr	r		150-210	0	0					
570	fS			gr	r		105-150	0	0					
580	fS			gr	r		105-150	0	0					
590	fS			gr	r		105-150	0	0					
600	fS			gr	r		105-150	0	0					
610	fS			gr	r		105-150	0	0					
620	fS			gr	r		105-150	0	0					
630	fS			gr	r		105-150	0	0					
640	fS			gr	r		105-150	0	0		13			
650	fS			gr	r		105-150	0	0					
660	fS			gr	r		105-150	0	0					
670	fS			gr	r		105-150	0	0					
680	fS			gr	r		105-150	0	0					
690	SCL			gr	r			0	0					
700	SC			gr	r			0	0					clay w/ sand layers
710	SC			gr	r			0	0					
720	SC			gr	r			0	0					
730	SC			gr	r			0	0					
740	SC			gr	r			0	0					
750	SC			gr	r			0	0					
760	SC			gr	r			0	0					
770	C			gr	r			0	0		14			
780	C			gr	r			0	0					
790	C			gr	r			0	0					
800	C			gr	r			0	0					
810	C			gr	r			0	0					
820	C			gr	r			0	0					
830	C			gr	r			0	0					
840	C			gr	r			0	0					
850	C			gr	r			0	0					
860	C			gr	r			0	0					
870	C			gr	r			0	0					
880	C			gr	r			0	0					
890	C			gr	r			0	0					
900	C			gr	r			0	0					
910	C			gr	r			0	0					
920	C			gr	r			0	0					
930	C			gr	r			0	0					some micas or shell frags
940	C			gr	r			0	0					
950	C			gr	r			0	0					
960	C			gr	r			0	0					(pic) coarse sand in clay
970	C			gr	r			0	0					
980	C			gr	r			0	0					
990	C			gr	r			0	0		15			
1000	C			gr	r			0	0					all cay or SiC, or mud?

End of borehole: 601901032